

June 21, 2023

Memo: SAG Recommendations for Establishing Emissivity Grids to be used in Modeling of Pre-Disturbance Conditions and Future Excess Emissions Reductions

From: Scientific Advisory Group (SAG)

To: Jon O'Brien, California Department of Parks and Recreation
Karl Tupper, San Luis Obispo Air Pollution Control District

Cc: Sarah Miggins, California Department of Parks and Recreation
Gary Willey, San Luis Obispo Air Pollution Control District

The recently revised Stipulated Order of Abatement (SOA), filed on October 18, 2022, requires that Annual Report and Work Plans (ARWP) submitted by the California Department of Parks and Recreation (CDPR) “**shall be designed to eliminate emissions in excess of naturally occurring emissions from the ODSVRA [Oceano Dunes State Vehicular Recreation Areas] that contribute to downwind violations of the state and federal PM₁₀ air quality standards**” (Section 3.b.), and that to meet this objective, CDPR “**shall initially reduce mass-based PM₁₀ emissions within the ODSVRA to a level consistent with the pre-disturbance scenario identified by the SAG [Scientific Advisory Group]**” (Section 3.c.). Taken together, these directives place a great deal of emphasis on dust emissions from the ODSVRA both past and present. ‘Past’ refers to expected baseline emissions from a pre-disturbance¹ state (i.e., prior to significant human impact, specifically from vehicular traffic) and ‘present’ refers to emissions from the contemporary landscape, including a combination of riding and non-riding areas.

Of course, past conditions are unknowable with absolute certainty. But sophisticated modeling with rational, scientifically-defensible assumptions, informed by historical reconstructions from aerial photographs of land cover change, can provide reasonable estimates of probable conditions on a natural or a potentially restored landscape absent of OHV traffic. Modeling of present conditions have the further advantage of complementary measurements that can be used to calibrate and validate the model results, thereby providing confidence in interpretation of contemporary processes of dust emission, transport, and dispersion from the ODSVRA.

A key component of representing and quantifying past and present air quality conditions is properly parameterizing the emissivity (dust-releasing nature) of sand surfaces within the ODSVRA dune landscape. To this end, the Desert Research Institute (DRI) has undertaken an

¹ It is recognized that human activities, including vehicular traffic, horse riding, hiking, and camping, have been a part of the Oceano Dunes landscape for many decades, prior to establishment of ODSVRA in the 1970s. There is very limited photographic evidence of landscape configuration prior to the early 1900s when human recreational activities began to influence the natural landscape. The earliest historical aerial photography from the 1930s reflects some level of disturbance, and as such, the term 'pre-disturbance' state is somewhat of a misnomer. Nevertheless, for consistency with the language used in the SOA regarding modeling of a pre-disturbance scenario, we will continue to use the term 'pre-disturbance' (as well as 'naturally occurring' emissions). As explained in the UCSB Vegetation Cover Analysis Report (February 2022), the 1939 imagery dataset is considered to be the best available indication of landscape configuration (i.e., vegetation cover, dune presence) prior to extensive Off-Highway Vehicle (OHV) activity within the Oceano Dunes.

extensive series of field campaigns since 2013 to measure surface emissivity using an instrument referred to as a “PI-SWERL (Portable In-Situ Wind EROsion Laboratory). DRI has reported on the results of these field campaigns, and most recently submitted another report entitled “**PI-SWERL September 2022 Results and Implications for Emission/Dispersion Modeling**” that describes the September 2022 PI-SWERL campaign. The 2022 field campaign quantified PM₁₀ emissivity in three zones of management that had not been previously measured: (1) new foredune restoration area (FRA); (2) the permanently exclosed Western Snowy Plover nesting area (PE), and (3) other seasonal exclosure (SE) areas. In the CDPR **2022 Annual Report and Work Plan (ARWP)**, all of these areas were identified as requiring further study to refine PM₁₀ emissions estimates via the DRI Emission/Dispersion Model (Mejia et al., 2019), with the goal of reporting updated modeling of PM₁₀ emissions for the 2023 ARWP (in progress). DRI made several recommendations regarding how to utilize the PI-SWERL data in future modeling scenarios, and Table 1 provides a summary.

Table 1: DRI proposed approaches to modeling PM₁₀ emissivity for specific dust control management areas not previously measured.

Dust control management area	Previous modeling approach (for 2022 ARWP)	Proposed new modeling approach (for 2023 ARWP)
Foredune restoration area	Use mean (average) 2019 PI-SWERL non-riding PM ₁₀ emissivity curve	Use mean (average) 2022 PI-SWERL measurements in foredune restoration area to create PM ₁₀ emissivity curve
Permanent plover exclosure	Use 50% of mean (average) 2019 PI-SWERL plover exclosure PM ₁₀ emissivity curve	Use mean (average) 2022 PI-SWERL measurements in plover exclosure to create PM ₁₀ emissivity curve
Seasonal beach exclosures	Use mean (average) 2019 PI-SWERL non-riding PM ₁₀ emissivity curve	Use mean (average) 2022 PI-SWERL measurements in the seasonal beach exclosure area to create PM ₁₀ emissivity curve
Seasonal transportation corridor exclosures	Use mean (average) 2019 PI-SWERL non-riding PM ₁₀ emissivity curve	Use mean (average) 2022 PI-SWERL measurements in seasonal corridors to create PM ₁₀ emissivity curve

The DRI 2022 PI-SWERL report was reviewed but not yet endorsed by the SAG (**SAG Review of Desert Research Institute (DRI) report, “PI-SWERL September 2022 Results and Implications for Emission/Dispersion Modeling”**, February 10, 2023). SAG members made several recommendations for clarification and improvement of the report. One area of concern was with regard to the specifics of the emissivity grids that DRI proposed to use in updated modeling runs. The SAG review indicates the following points of clarification (reproduced verbatim with italics added):

(1) Underlying emissivity grid. The use of an amalgamated 2013-2019 PI-SWERL emissivity grid for the pre-disturbance scenario, versus use of the 2019 PI-SWERL emissivity grid for mitigation scenarios, is potentially an “apples-to-oranges” comparison that needs to be further justified. The issue is that the 2013 PI-SWERL grid, used as the “baseline year” under the previous terms of the SOA, appears to display anomalously high PM₁₀ emissivity as compared to any other year or long-term trend. By including 2013 emissivity data for the baseline and pre-disturbance scenario, CDPR may therefore be claiming credit for a greater percentage emissions reduction than is actually merited. (See comment “C” in SAG review of 2022 ARWP.)

On October 21, 2022, the San Luis Obispo County Air Pollution Control District (SLOAPCD) conditionally approved the 2nd Draft 2022 Annual Report and Work Plan (SLOACPD, 2022). However, the SLOAPCD shared many of the SAG’s concerns about modeling assumptions, which may be crediting CDPR dust mitigation measures with achieving a greater level of PM₁₀ emissions reductions than may actually be merited. Therefore, as the condition for its approval of the 2022 ARWP, SLOAPCD mandated that these model issues be addressed in the 2023 ARWP. SLOAPCD’s conditional approval letter stated, “Emission calculations in the 2023 ARWP shall be based on assumptions recommended by the SAG and preapproved, in writing, by the APCO.”

The purpose of this memorandum is to present a comprehensive analysis of the existing PI-SWERL data of actual dust emissivity within ODSVRA, and to make recommendations regarding an emissivity grid that could be incorporated into future modeling efforts leading to implementation of the excess emissions framework proposed by SAG (**SAG Memo – Framework for Assessing “Excess Emissions” of PM₁₀ from the Oceano Dunes**, January 30, 2023), thereby satisfying the requirement of the conditional approval letter. Model updates are also important for the purpose of quantifying changing emission conditions due to mitigation strategies undertaken within the yearly ARWPs.

The analysis of the PI-SWERL data is broken into several distinct sections appended to this memo below, which concludes with recommendations for the proposed emissivity grid.

Respectfully,

The Scientific Advisory Group²

Bernard Bauer (Chair), Carla Scheidlinger (Vice-Chair), Mike Bush, Jack Gillies, Jenny Hand, Leah Mathews, Ian Walker

² As a co-author of the DRI 2022 PI-SWERL report, SAG member John A. Gillies did not contribute to the review of the report, but was part of the discussions leading to the recommendations in this memorandum. Although Raleigh Martin (former SAG Chair) recently left SAG, he provided a substantive review of this memorandum, having had a lengthy engagement with the particulars of the emissivity grids that constitutes invaluable knowledge. His efforts are warmly acknowledged.

OVERVIEW OF PI-SWERL MEASUREMENTS

DRI began collecting PI-SWERL data in August, 2013, and have conducted measurement campaigns for most years up to September, 2022. The PI-SWERL instrument and its field application have been described extensively in numerous publications (e.g., Mejia et al., 2019 and references therein). The PI-SWERL data are generally categorized as either Riding Area (RA) or Non-Riding Area (NRA). **A total of 1516 distinct measurement locations have been sampled (Table 2), with sampling in the RA prioritized over the NRA at a split of 984 to 532. An additional 69 PI-SWERL measurements were taken in areas that are 'seasonally exclosed',** which means that riding is allowed during part of the year (October 1 through February 28) followed by a period of exclosure (March 1 through September 30) when riding is not allowed. These 69 measurements will be treated separately toward the end of this document.

Table 2: Summary of PI-SWERL Measurements at ODSVRA

YEAR_Month(s)	Riding Area	Non-Riding Area
2013_08	186	143
2014_09	45	35
2015_06	100	2
2015_9/10	165	6
2016_03	58	34
2019_05	337	124
2019_10	42	28
2022_05	51	27
2022_09		133
TOTAL	984	532

The footprint of the zones designated for riding and non-riding has evolved over time due to management interventions directed at dust mitigation. The majority of the land base has not changed designation, but significant acreage originally open for riding has transitioned to non-riding status, typically with fenced exclosures and surface treatments (i.e., straw, surface texturing, scattered seeds, and planted vegetation) or sand fencing. Thus, there are areas considered as 'transitional' because they have not had sufficient opportunity to revert to naturalized conditions and may be displaying residual effects from OHV riding. As an example, the Foredune Restoration Area (FRA) was exclosed in December, 2019 and, prior to that date, this zone was accessible to OHV traffic and camping activities. A total of 71 measurements were taken in this zone while it was designated as RA, and 110 measurements were taken in September, 2022, 31 months (~2.5 years) following implementation of restoration treatments in February, 2020. The data from the FRA are included in the summary values presented in Table 2, but the FRA will be treated separately for purposes of modeling. The same situation applies to the Western Snowy Plover Exclosure (PE), which was seasonally accessible to OHV use during the non-nesting/rearing season (October through February, inclusive) but is now permanently closed. As mentioned above, there is a relatively small area (34.6 acres) that is currently

managed for both OHV access and seasonal exclusion during different times of the year, and since it is neither fully riding nor non-riding, as are other parts of the ODSVRA, it will be assessed separately (and is not included in Table 2).

Due to logistical challenges associated with changes in surface cover, dune movement, evolving restoration treatments and habitat protection, the PI-SWRL measurements are not equally distributed over time or in space. Rather, the sampling design from year-to-year addressed strategic operational needs (e.g., parameterizing the zones most likely to influence air quality or identifying areas for management interventions) rather than statistical requirements (e.g., quantifying uncertainty). Therefore, the sampling approach was neither (stratified) random nor regularly spaced. Moreover, access to certain locations is restricted during certain times of the year because of regulations regarding protected species (e.g., Snowy Plover, California Least Tern). Nevertheless, the large number of measurements within the ODSVRA in both riding and non-riding areas ensures that statistical testing can be conducted with some degree of confidence in the results. **When interpreting the results, however, it is important to appreciate that there may be some sampling bias with respect to either time or space depending on how the data are clustered when assessing group differences or similarities.** The following two sections deal with the temporal and spatial elements of the PI-SWRL measurements independently.

TEMPORAL DIMENSIONS OF PI-SWRL SAMPLING

It is to be expected that there will be seasonal influences on dust emissions from the ODSVRA because of weather-related (i.e., moisture, temperature, windiness) differences between spring (wet) and fall (dry) conditions. In addition, the intensity of OHV traffic and camping use varies during the year. In an attempt to tease out some of these influences, the PI-SWRL measurement results from the Riding Area (RA) were disaggregated according to month/year of sampling and represented using box-and-whisker plots (Figure 1).

A Theil trend analysis (Wilcox, 2005) resulted in no statistically significant trends ($p < 0.01$) in emissivity over time for any of the percentiles shown in the panels in Figure 1 (see Appendix 1 for analysis results). The relatively large dust emissions during the 2013 campaign were noted previously (e.g., 2022 ARWP, Section 2.3.5.1; https://storage.googleapis.com/slocleanair-org/images/cms/upload/files/2ndDraft2022ARWP_2022914.pdf) and were likely due to an extended drought in California (2011-2017); 2013 was a particularly dry year (<https://weather.com/news/news/much-california-2013-was-driest-year-record-20140101>). Moreover, the 2013 campaign was conducted in August, which is characteristically dry, as well as coinciding with intense OHV use of the park. Nevertheless, inclusion of the 2013 data in the regression did not change the final result that there was no significant temporal trend.

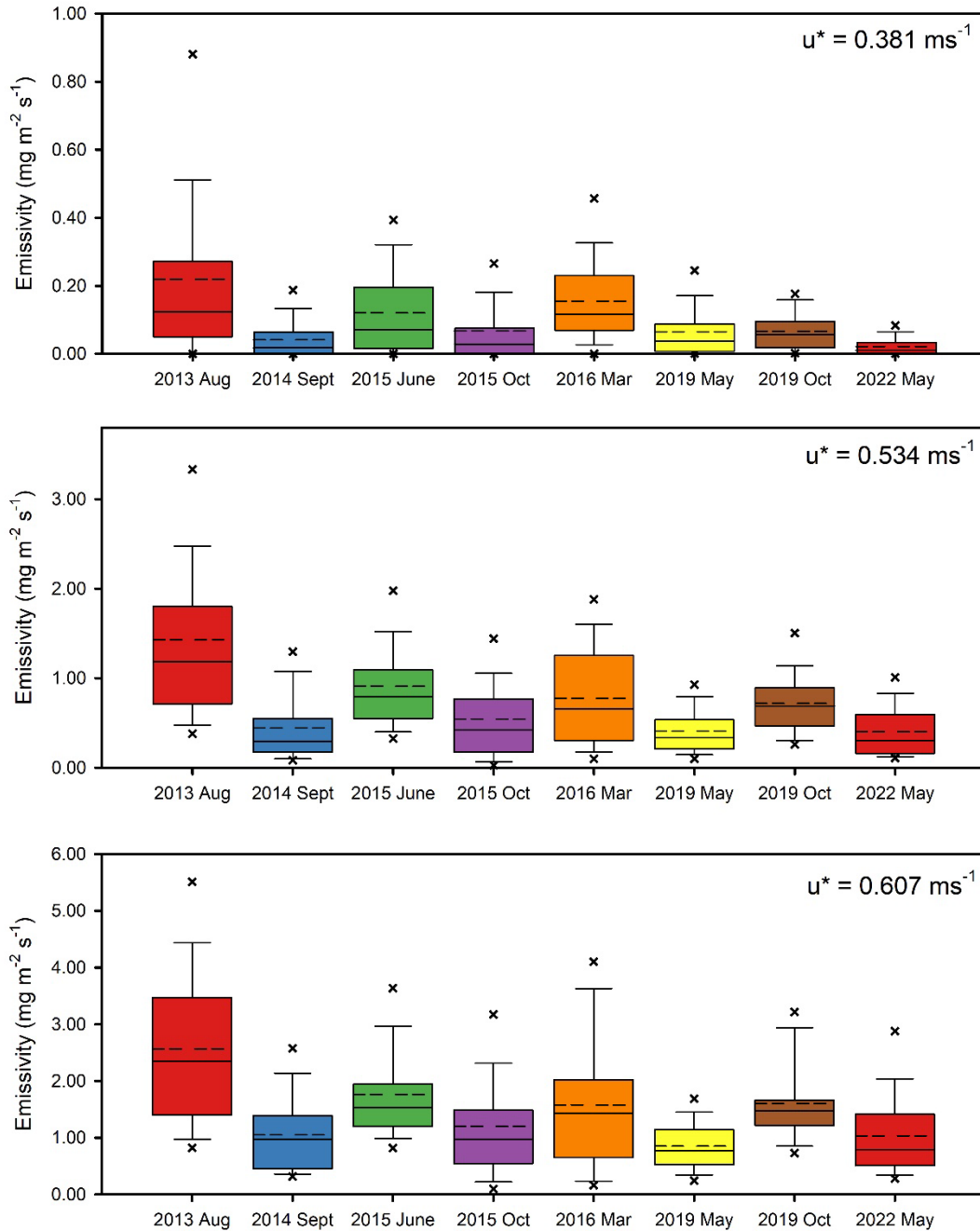


Figure 1: Box-and-whisker plots of PI-SWERL measurements made in the Riding Area (RA) from each field campaign from 2013 through 2022. The colored boxes define the range of the 25th and 75th percentiles; the whiskers correspond to the 10th and 90th percentiles; and the outer symbols (x) indicate the 5th and 95th percentiles. The median value is given by the horizontal solid line within the box, whereas the arithmetic mean (average value) is shown by the horizontal dashed line. The three panels correspond to the three RPM speeds used in the PI-SWERL device to characterize dust emissions at any single measurement location.

Figure 2 shows summary results from an Analysis of Variance (ANOVA) on Ranks using Dunn’s test, which is a nonparametric test that does not require equal sample sizes or assuming that all samples were drawn from normally distributed populations with equal variances. Invoking Dunn’s test was necessary because none of the measurement campaigns yielded emissivity distributions that were normally distributed. The significance level for all ANOVA on Ranks tests in this report was $p < 0.01$. The results show that the August 2013 data ($n = 186$) are significantly different from most other years (indicated by red boxes), with the exception of June 2015 ($n = 100$) and October 2019 ($n = 42$), which are not statistically different. Overall, it appears as if the lower emissivity periods (September 2014, October 2015, May 2019, and May 2022) are statistically similar to each other but different from the higher emissivity periods (June 2015, March 2016, and October 2019). Of interest for the purposes of this temporal analysis is the fact that there were two measurement campaigns in 2015 (June and October) and in 2019 (May and October), with the June 2015 campaign having greater overall emissivity than in October 2015, whereas the opposite is true for the May 2019 and October 2019 campaigns. As noted earlier, it is important to keep in mind that field campaigns in different years/seasons had different areal coverage, varying sample sizes, and did not regularly re-occupy the same locations, which makes a temporal analysis challenging. Developing a sampling framework that would allow a robust statistical analysis of ODSVRA emissivity data is a challenge due to its size, temporal changes in emissivity on multiple scales, the logistical difficulties of measurement campaigns, and the expense of those campaigns.

Riding Area	Aug 2013	Sep 2014	Jun 2015	Oct 2015	Mar 2016	May 2019	Oct 2019	May 2022
Aug 2013	-							
Sept 2014	Y	-						
Jun 2015	N	Y	-					
Oct 2015	Y	N	Y	-				
Mar 2016	Y	N	N	N	-			
May 2019	Y	N	Y	Y	Y	-		
Oct 2019	N	Y	N	Y	N	Y	-	
May 2022	Y	N	Y	N	N	N	Y	-

Figure 2: Summary results from ANOVA on Ranks test to determine whether there are significant differences ($P < 0.01$) between measurement results from different campaigns for the Riding Area. Boxes in red with 'Y' indicate that there are significant differences between the two sets of data (column vs row) whereas boxes in green with 'N' indicate that the data sets are not statistically different. This analysis considers only the high RPM ($u^* = 0.61 \text{ m s}^{-1}$) PI-SWERL data, but the other two sets of data (low and mid RPM) produced similar results.

Figure 3 shows box-and-whisker plots of the PI-SWERL measurement results from the Non-Riding Area (NRA) disaggregated according to year/month of sampling. As with the RA data, Theil regression demonstrated that there is no statistically significant temporal trend (Appendix 1). Relatively low emissivity values occurred in the two 'transitional' areas—i.e., the Foredune Restoration Area (FRA) and the permanent Plover Exclosure (PE). The March 2016 data (n = 34) had the largest mean and median values, whereas the October 2019 data (n = 28) had the smallest mean and median (aside from the 2015 measurements with an n = 8 when the June and October data were clustered). The May 2022 data (n = 27) show an increase in emissivity relative to the October 2019 low.

Figure 4 shows the results of the ANOVA on Ranks tests for the Non-Riding Area campaigns. The 2015 data set was excluded from this analysis because it comprised only 8 measurements in the Non-Riding Area. Many of the data sets from individual years are statistically different from each other. Of interest is that the August 2013 data set is different from most others with the exception of the two sampling campaigns immediately following (2014 and 2016). The October 2019 campaign appears to be a 'swing' year, being statistically different from earlier campaigns but not different from later campaigns. Also, of note is that the May 2022 data set cannot be considered statistically different from most other years with the exception of August 2013 (much higher emissivity). Moreover, the May 2022 data for the NRA are also statistically different from both the Foredune Restoration Area and Plover Exclosure, both of which were measured later in the same year and have very low emissivity.

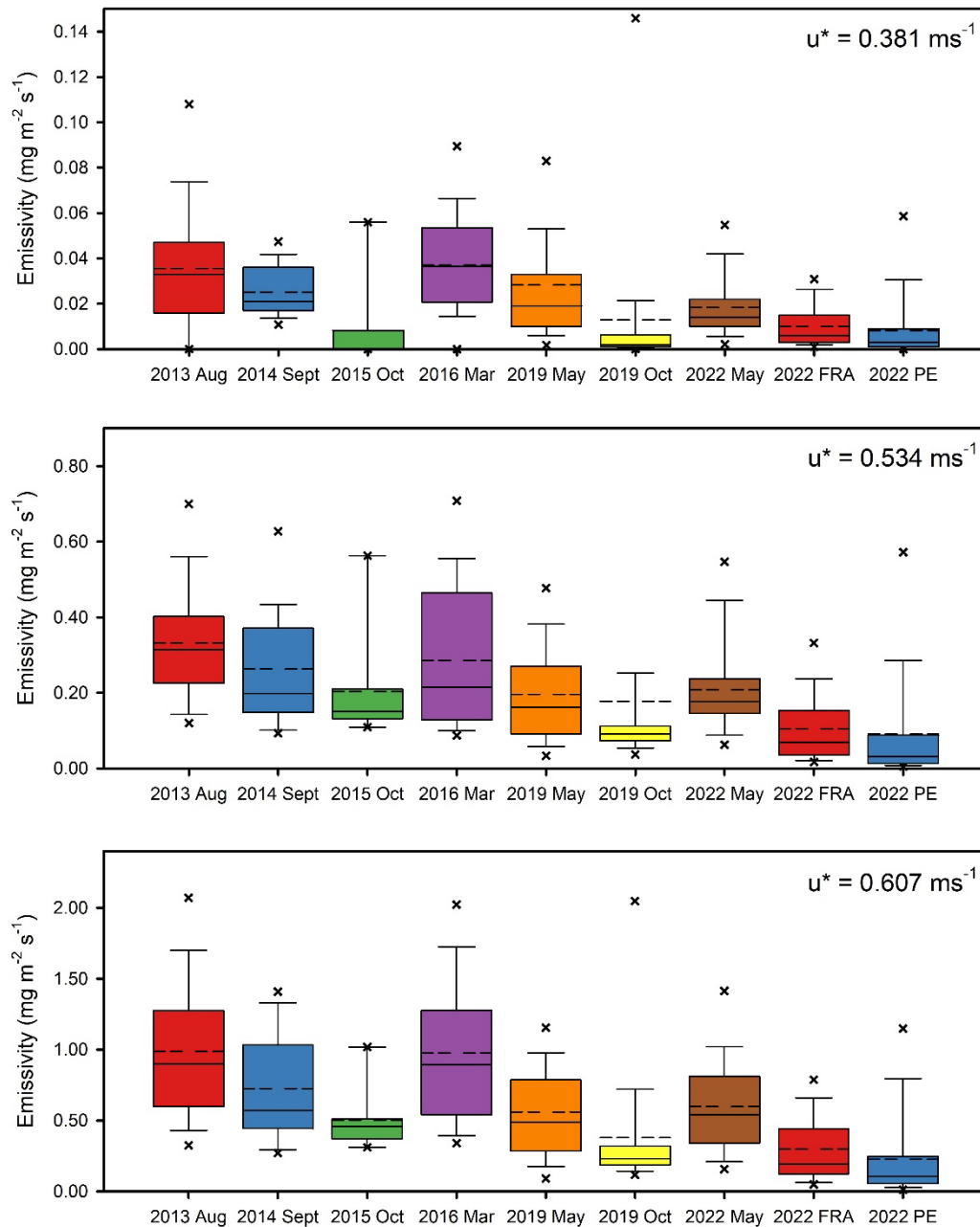


Figure 3: Box-and-whisker plots of PI-SWERL measurements made in the Non-Riding Area (NRA) from each field campaign from 2013 through 2022. The colored boxes define the range of the 25th and 75th percentiles; the whiskers correspond to the 10th and 90th percentiles; and the outer symbols (x) indicate the 5th and 95th percentiles. The median value is given by the horizontal solid line within the box, whereas the arithmetic mean (average value) is shown by the horizontal dashed line. The three panels correspond to the three RPM speeds used in the PI-SWERL device to characterize dust emissions at any single measurement location. “FRA” refers to Foredune Restoration Area; “PE” refers to Plover Exclosure.

Non-Riding Area	Aug 2013	Sep 2014	Mar 2016	May 2019	Oct 2019	May 2022	Sep 2022 FRA	Sep 2022 PE
Aug 2013	-							
Sept 2014	N	-						
Mar 2016	N	N	-					
May 2019	Y	N	Y	-				
Oct 2019	Y	y	Y	N	-			
May 2022	Y	N	N	N	N	-		
Sep 2022 FRA	Y	Y	Y	Y	N	Y	-	
Sep 2022 PE	Y	y	Y	y	N	y	N	-

Figure 4: Summary results from ANOVA on Ranks test to determine whether there are significant differences between measurement results from different campaigns for the Non-Riding Area. Boxes in red with 'Y' indicate that there are significant differences between the two sets of data (column vs row) whereas boxes in green with 'N' indicate that the data sets are not statistically different. FRA means foredune restoration area; PE means permanent plover exclosure. This plot considers only the high RPM ($u^* = 0.61 \text{ m s}^{-1}$) PI-SWERL data, but the other two sets of data (low and mid RPM) produced similar results.

This initial statistical assessment suggests that, despite notable temporal variability in the RA and NRA data, there is no statistically significant temporal trend in emissivity. Part of this outcome relates to the fact that moisture and temperature conditions are highly variable in coastal areas, yet the PI-SWERL sampling strategy does not, and logistically is unable to, control for this variability. Surface moisture conditions can change hourly, daily, weekly, monthly, seasonally, and inter-annually, and it would require a significantly more intensive effort to account for surface moisture conditions in relation to precipitation, relative humidity, and temperature changes. Moreover, there may be a co-dependency on the spatial distribution of measurements from year-to-year, which will be considered next.

SPATIAL DIMENSIONS OF PI-SWERL SAMPLING

The PI-SWERL data were imported into an open-source geographic information system (QGIS) to render a spatial view of the sampling locations. Figure 5 shows the measurement locations relative to the park boundaries. Most areas have been sampled extensively although there are certain areas where the density of points is much greater than in others. The FRA, for example, has a relatively large density of measurements, the majority of which (110 of 181 points) were

collected in September 2022 after 33 months (~2.75 years) of exclosure to OHV access. The PE, in contrast, has relatively few points given the large size of the area, and all these measurements were made in September 2022. There are no measurements in this area during the period when it was seasonally open for OHV riding. The sampling strategy in the PE appears to have followed a longitudinal north-south transect along the middle of the preserve, with points in the north being slightly closer to the shore than points in the south where the exclosure is wider. Many of the other data points in the rest of the park follow west-east transects that run parallel with the prevailing (effective) wind direction out of the WNW.

The points in Figure 5 are color-coded to reflect the date of the measurement campaign (browns indicating older measurements taken in 2013-2015, neutral colors indicating mid-decade, and blue colors indicating recent measurements). Many points are not visible in this graphic either because the sampling was performed in tight spatial clusters or because multiple measurements in different years fall in approximately the same location (i.e., the symbols are stacked with only the most recent appearing on the map).

Figure 6 shows the same data but disaggregated according to year of the field campaign (measurements made between 2014 and 2016 are represented on one map because of the relatively small number). Despite the multitude of measurements covering most of the area of the ODSVRA, it is evident that the sampling was performed unevenly, both temporally and spatially, as mentioned earlier. The two largest field campaigns were in 2013 (RA n=186; NRA n=143) and 2019 (RA n=379; NRA=152) with measurements spanning most of the park. The Dune Preserve to the north (also an NRA) was sampled intensely in 2013 covering most of the area and was revisited in 2019 to duplicate two of the transects. A similar sampling approach was taken to the south in the Oso Flaco NRA zone with intense sampling in 2013 and re-sampling of a west-east transect in 2019.

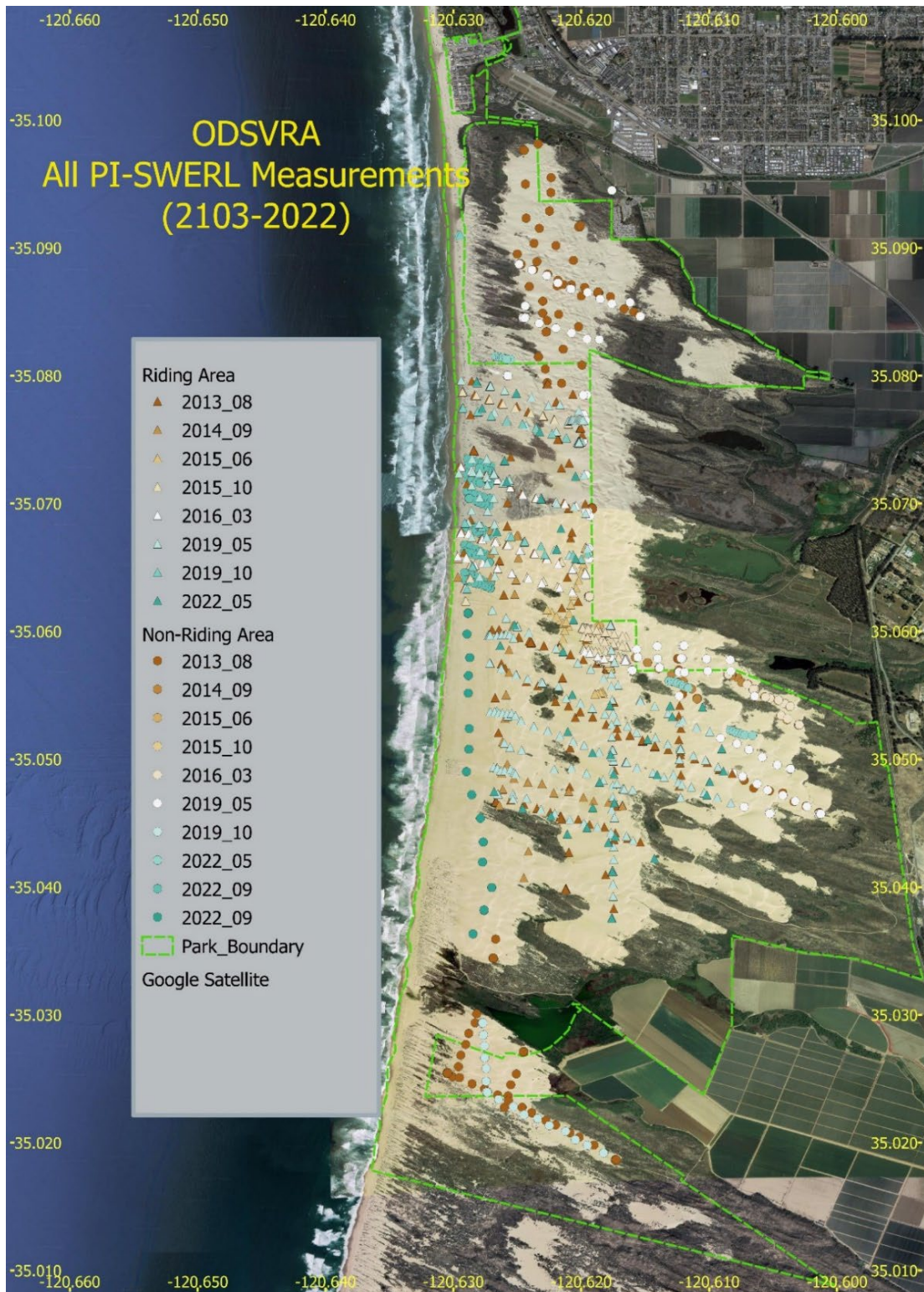


Figure 5: Location of all PI-SWERL measurements from 2013 to 2022. Triangles designate samples taken within the Riding Area (OHV accessible) and circles designate Non-Riding Area samples. Samples in the Seasonal Exclusion area from 2022 are not shown.

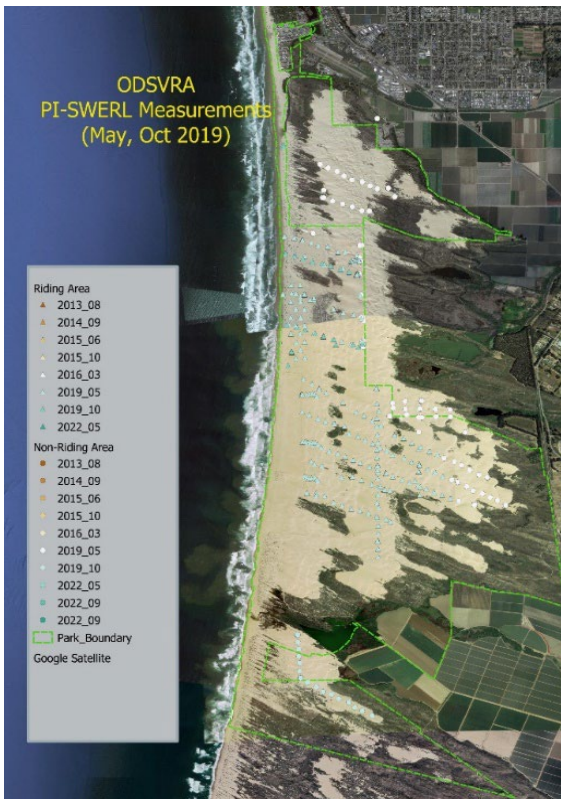
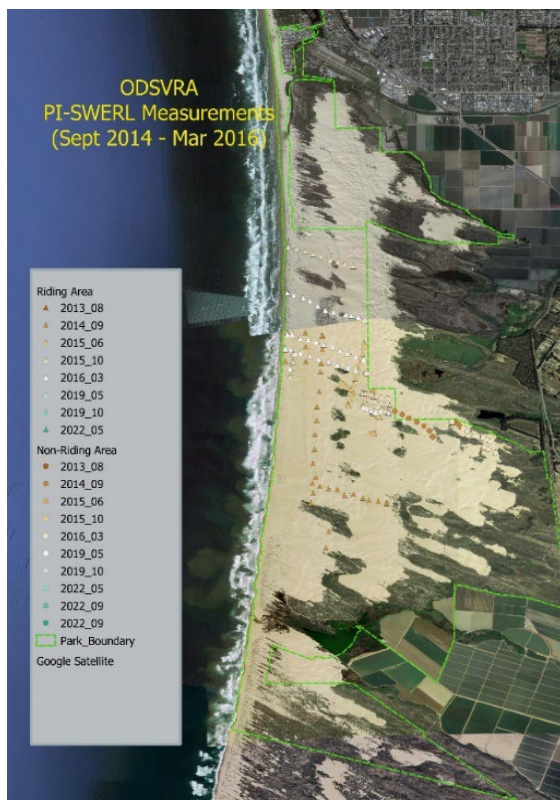
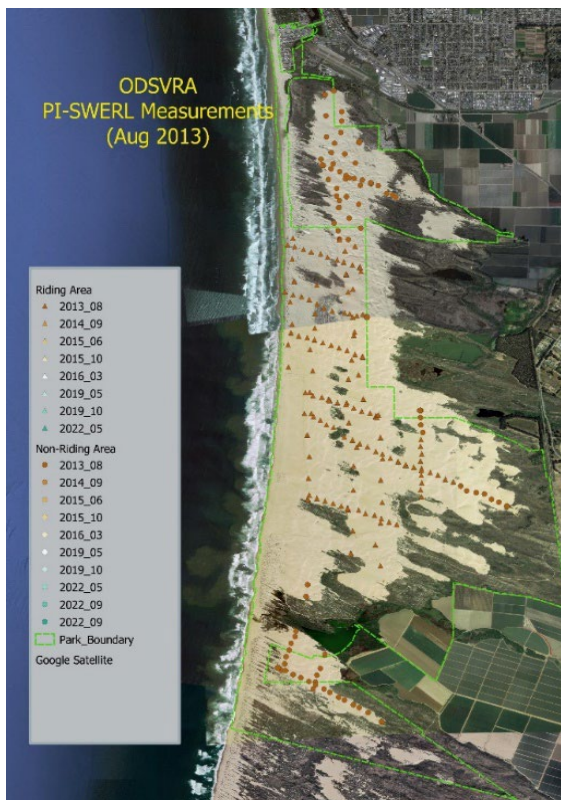


Figure 6: Location of PI-SWERL measurements during different field campaigns from 2013 to 2022. Triangles designate Riding Area and circles designate Non-Riding Area.

The measurements from 2014-2016 were focused on the central region, largely targeting the Riding Area upwind of the CDF and Mesa2 air quality monitoring stations. Measurements in 2022 also focused on the central region with prioritization of the FRA, PE, the SE areas, and the RA. There were no PI-SWERL measurements collected in 2017, 2018, 2020, and 2021.

As noted in the previous section, there were no discernable long-term trends in the PI-SWERL data. A more thorough statistical investigation is hampered by the fact that the sampling design did not call for replication of measurement locations across multiple years (except for a few instances where certain transects were re-occupied in different years, e.g., 2013 and 2019). Therefore, there is an added spatial dimension to consider to the data distributions. It has been suggested, for example, that due to mean grain size increases from north to south (see Scientific Advisory Group Report, February 2023, *Oceano Dunes: State of the Science*) there may be a corresponding decrease in dust emissions from north to south. This possibility was recognized in earlier modeling efforts by DRI, and this will be considered for both the RA and NRA data below.

When examining the spatial distribution of the Non-Riding Area measurements, it becomes clear from Figures 5 and 6 that there are three distinct zones: (1) the Dune Preserve to the north (demarcated by N 35.0794° latitude as the southern boundary, which is slightly south of the park boundary); (2) a Southern Zone falling to the south of the Plover Enclosure and the riding area (referred to as Oso Flaco); and (3) a Central Zone that covers all the remaining area in between these lines of latitude. The PI-SWERL measurements were clustered into these three zones for statistical analysis, with the exception that the data from the Foredune Restoration Area and the Plover Enclosure were kept aside and treated independently.

Figure 7 shows box-and-whisker plots for the North, Central, and South zones as well as the FRA and PE zones, retaining the year of collection as an additional variable. Visually, the emissivity values to the south are generally smaller than the north, despite considerable scatter. The data from 2013, for example, stand out as having comparatively large emissivity relative to other years, especially in the North and South zones. In the Central zone, this difference is not quite as apparent because the data from 2016 (brown bar) have a very wide distribution despite a relatively small sample size (n=34). Approximately one third of these measurements were taken directly east of the fence that marks the riding area, whereas the remainder were taken just south of Black Lake (west of Callender) and far from the riding area. Once again, the measurements from 2015 (yellow bar) can be discounted because of small sample size (n=8).

For the purposes of testing whether there is indeed a north-south trend in emissivity, the data from each of the three zones were clustered (i.e., combining data from all years). The resulting box-and-whisker plots are shown in Figure 8. From this rendering, it becomes much clearer that **there is indeed a reduction in emissivity from north to south. In addition, the FRA and PE also show very low emissivity in comparison to the Central and North zones.** The ANOVA on Ranks results (for the high RPM case) are shown in Figure 9, from which it is evident that the groupings are all statistically different with one exception--the FRA measurements cannot be considered to be statistically different from the PE measurements, but they are both different from the South, Central, and North zones.

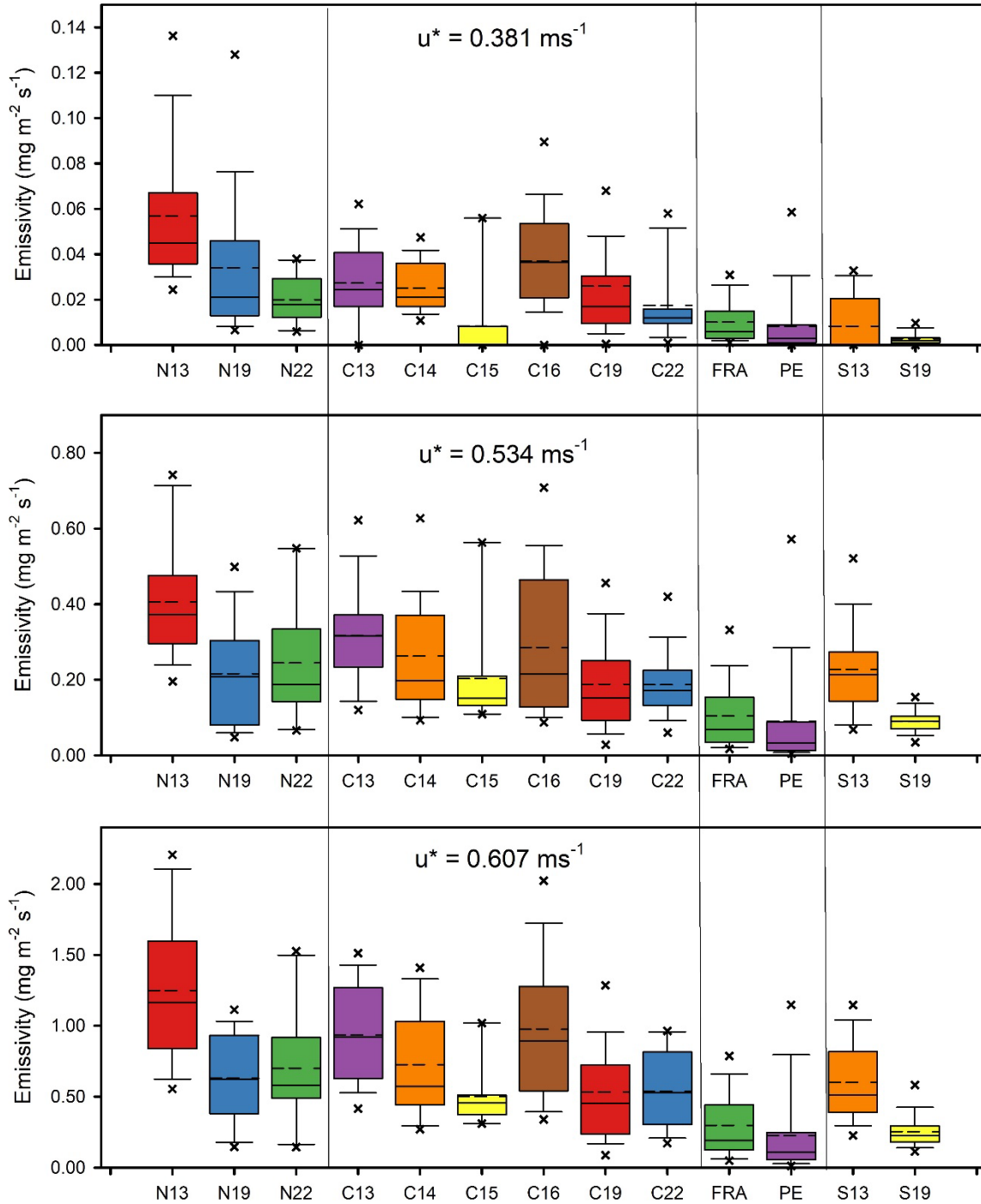


Figure 7: Box-and-whisker plots of PI-SWERL measurements made in the Non-Riding Area (NRA) from each field campaign from 2013 through 2022 disaggregated into North, Central, and South zones (delineated by vertical thin lines). Foredune Restoration Area (FRA) and Plover Exclosure (PE) are treated separately. See Figure 1 for explanation of symbols. The three panels correspond to the three RPM speeds used in the PI-SWERL device to characterize dust emissions at any single measurement location.

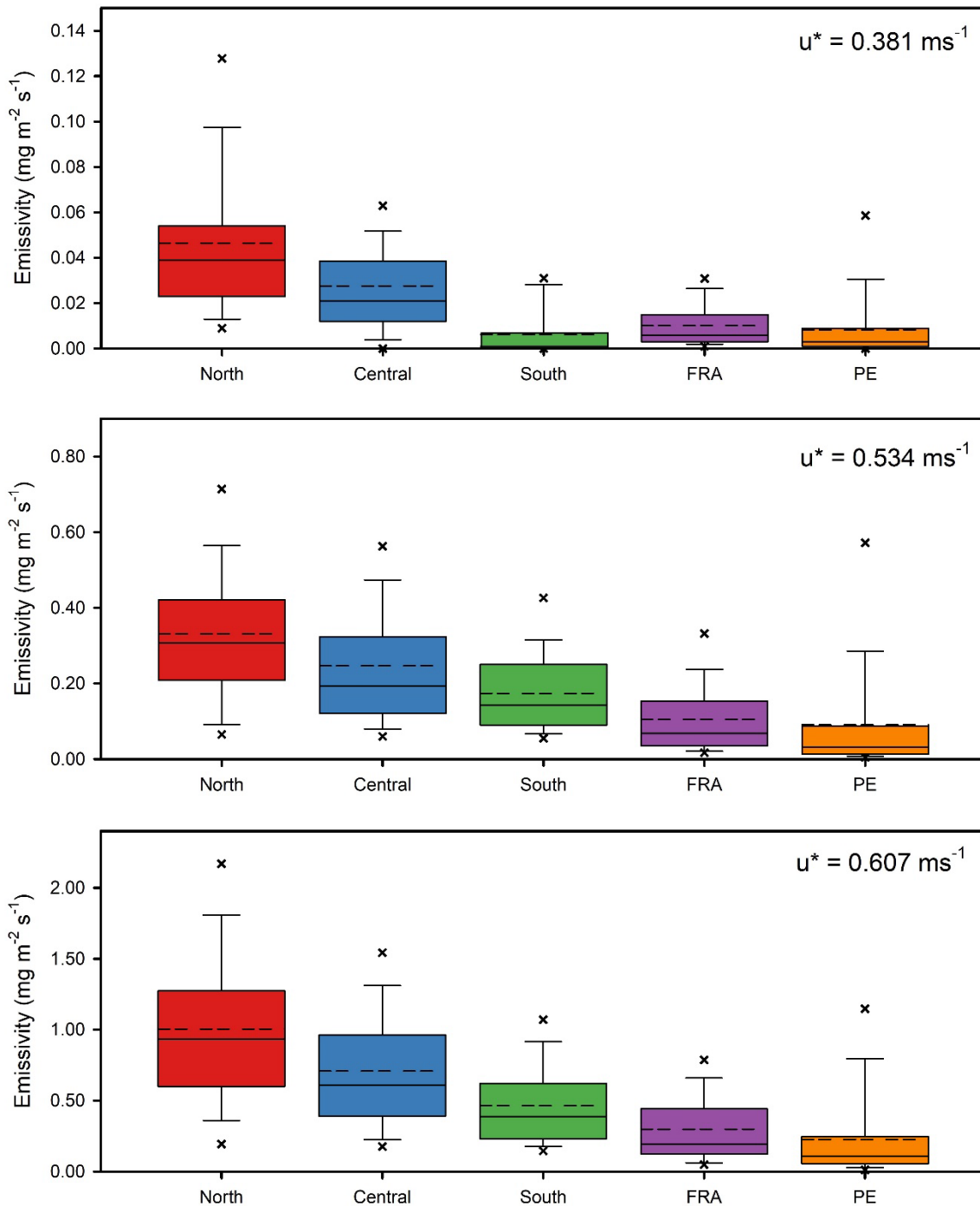


Figure 8: Box-and-whisker plots of PI-SWERL measurements made in the Non-Riding Area (NRA) aggregated into North, Central, and South zones. Foredune Restoration Area (FRA) and Plover Exclosure (PE) are treated separately. See Figure 1 for explanation of symbols. The three panels correspond to the three RPM speeds used in the PI-SWERL device to characterize dust emissions at any single measurement location.

Non-Riding Area	North	Central	South	FRA	PE
North	-				
Central	Y	-			
South	Y	Y	-		
FRA	Y	Y	Y	-	
PE	Y	y	y	N	-

Figure 9: Summary results from ANOVA on Ranks test to determine whether there are significant differences between measurement results for the Non-Riding Area clustered into zones in the north-south direction. Refer to Figure 7 for zones. Boxes in red with 'Y' indicate that there are significant differences between the two sets of data (column vs row) whereas boxes in green with 'N' indicate that the data sets are not statistically different. This plot considers only the high RPM ($u^* = 0.61 \text{ m s}^{-1}$) PI-SWERL data, but the other two sets of data (low and mid RPM) produced similar results.

Although an analysis of potential west-east trends was undertaken for the NRA data, the differences were not as apparent as for the north-south trends. Moreover, there is considerable subjectivity with regard to placement of separation boundaries for data aggregation, so this line of inquiry was not pursued further.

The Riding Area data shown in Figure 5 were all located within the central zone that was defined for the NRA data, and there are no obvious break points to create zones for the RA as was the case for the NRA. **The RA data were plotted according to latitude (Figure 10) to determine whether there was visual evidence to justify a separation. There is an evident decrease in emissivity toward the south, which is gradual but progressive.** The resulting R^2 values for the regression suggest that latitude is a weak explanatory variable given how much scatter there is at any single line of latitude. The scatter is skewed to much larger emissivity values in the north where the OHV use is more intense and spatially constrained than in the south. Visually, there appears to be a break at about $N 35.062^\circ$, which aligns roughly with the northern boundary of the PE and follows a parallel trajectory inland. The sub-region to the north of this line has characteristically larger emissivity values and large scatter than the sub-region to the south of this line.

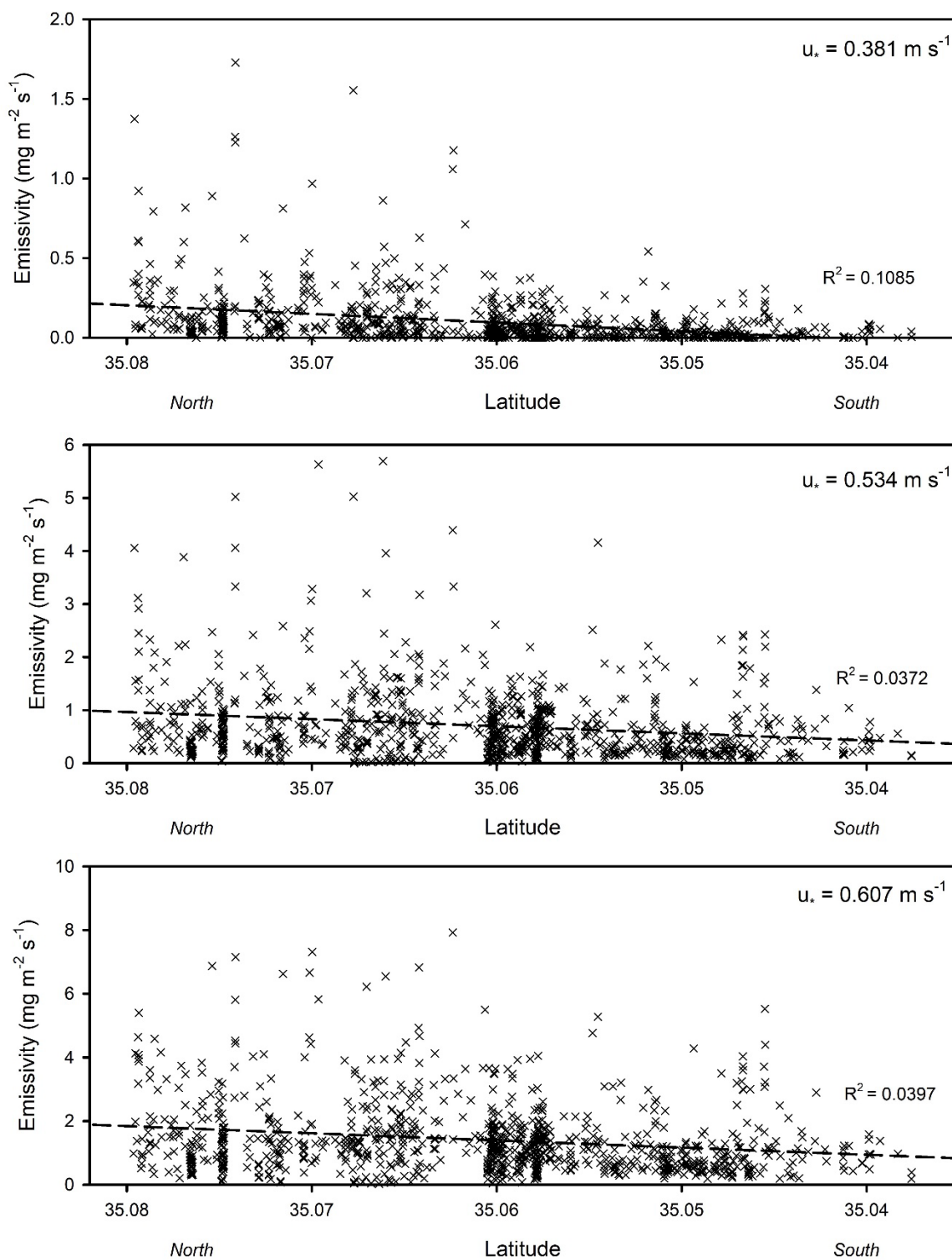


Figure 10: North-South trend in emissivity for Riding Area PI-SWERL data from 2013-2022. Dashed line is the best-fit linear regression line with R² values shown in each panel.

Following on the visual cues from Figure 10, the PI-SWERL RA data were pooled into two sub-regions (Central-North and Central-South) for additional analysis. Figure 11 provides the box-and-whisker plots that graphically portray the data distributions in each zone. Although the Central-South sub-region has generally smaller emissivity values, there is considerable overlap in the distributions. The Mann-Whitney Rank Sum Test was performed on the three sets of PI-SWERL data corresponding to the Lo-, Mid-, and Hi-RPM measurements to determine whether the data from the Central-North sub-region were statistically different from the Central-South sub-region. The results are provided in Table 3, and the very small p value indicates that the null hypothesis (no difference in samples) is to be rejected. Thus, there is a significant difference between the paired sub-regions. As with the NRA data, the analysis of west-east trends proved less revealing.

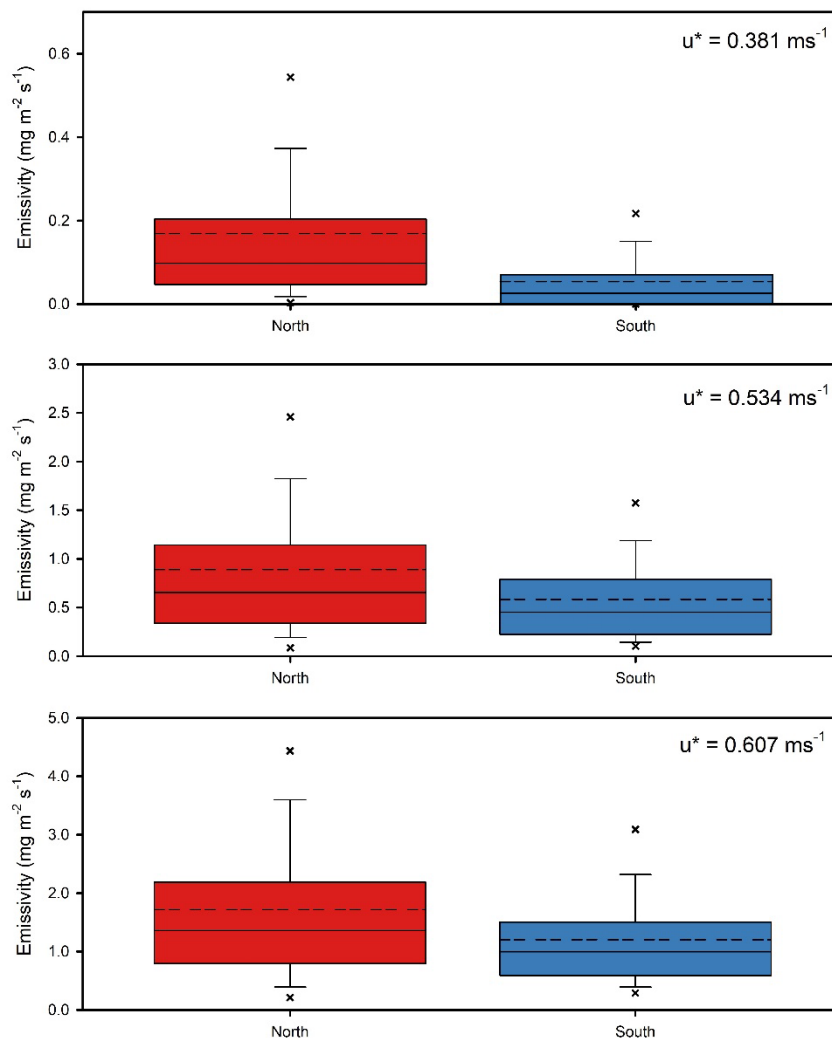


Figure 11: Box-and-whisker plots of PI-SWERL measurements made in the Riding Area (NA) aggregated into Central-North and Central-South sub-regions See Figure 1 for explanation of symbols. The three panels correspond to the three RPM speeds used in the PI-SWERL device to characterize dust emissions at any single measurement location.

Table 3: Results from Mann-Whitney Rank Sum Tests on PI-SWERL data from the Central-North (CN) and Central-South (CS) sub-regions of the Riding Area (2013-2022).

u* (m s⁻¹)	Median Emissivity (mg m⁻² s⁻¹)		U statistic	T value	p
	CN (n = 415)	CS (n = 569)			
0.381	0.098	0.026	56,062	264,422	< 0.001
0.534	0.655	0.454	89,606	229,900	< 0.001
0.607	1.360	0.996	88,582	224,646	< 0.001

RECOMMENDATIONS LEADING TOWARD MODEL EMISSIVITY GRIDS

Spatial Sub-Division (Zones and Sub-Regions)

The above analysis of the PI-SWERL data collected between 2013 and 2022 suggests that the **Riding Area** can be subdivided in two sub-regions (Central-North and Central-South) while the **Non-Riding Area** can be subdivided into three zones (North, Central, and South). Figure 12 shows these five primary areas as well as two additional areas designated as non-riding: (i) Foredune Restoration Area; (ii) Plover Exclosure, and the areas managed for Seasonal Exclosure (SE). The vegetated zones should be treated separately by overlaying a cover mask on the GIS model. Each of the zones and sub-regions are then allocated different emissivity characteristics for purposes of future dust emissions modeling.



Figure 12: Proposed zonation for disaggregating the PI-SWERL measurements (2013-2022) into three zones for the Non-Riding Area (NRA North, NRA Central, NRA South, separated by purple and blue dashed lines) and two sub-regions for the Riding Area (RA Central-North, RA Central-South separated by orange dashed line). Also shown are the boundaries of the Foredune Restoration Area (FRA), the Plover Exclosure (PE), and the Seasonal Exclosure (SE) areas. The current extent of the Riding Area is mapped in a light tan color. See also Figure 17.

The following recommendations are made with regard to the zonation of the ODVSRA, based on the PI-SWERL analysis presented above:

For the Riding Area, the Central-North and Central-South sub-regions should be delineated by a separation line that parallels the northern fenced boundary of the Plover Exclosure from the beach inland, and then following N 35.062° latitude past the eastern park boundary (Figure 13) to the end of the modeling domain. The northern and southern boundaries of the Riding Area are the same as the boundaries for the Non-Riding Areas, as described below.

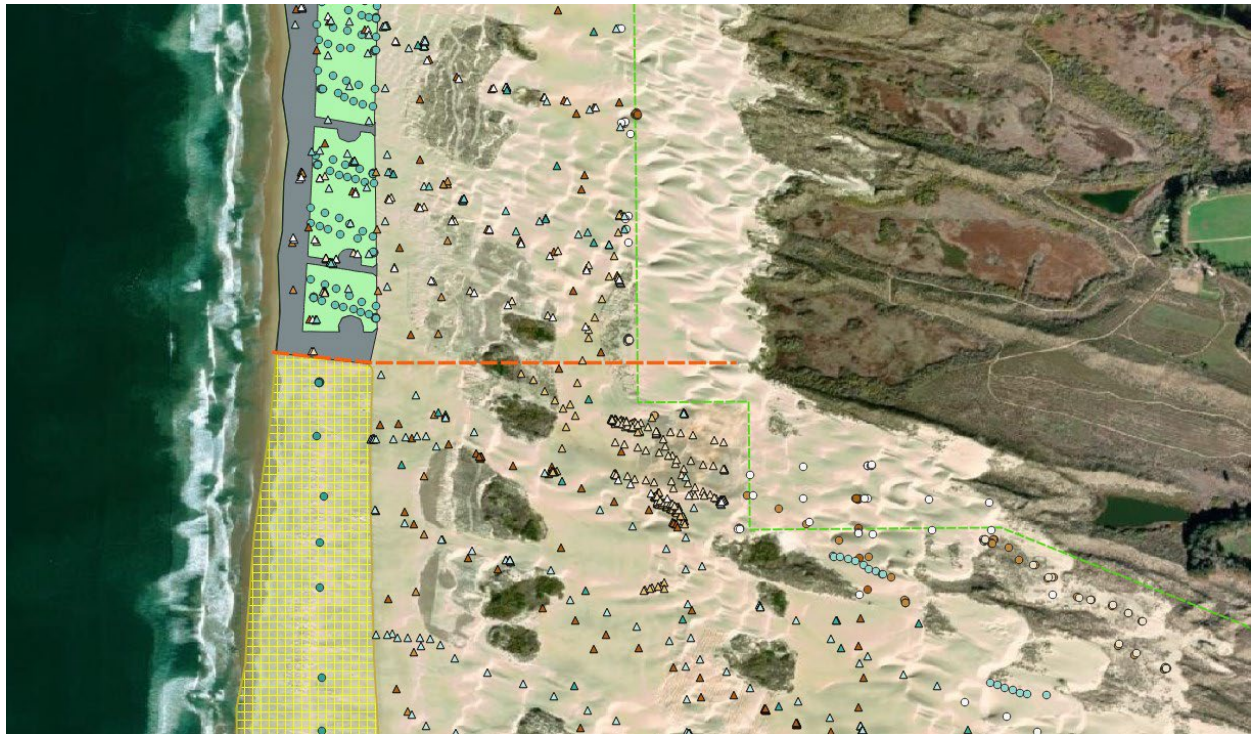


Figure 13: Proposed boundary line (orange dashed line) between the Central-North and Central-South sub-regions of the Riding Area. Refer to Figure 12 for location, and see Figure 5 for definition of symbols.

For the Non-Riding Area, three zones were identified (North, Central, South) from the statistical analysis. Figure 12 shows an overview of the recommended boundaries for these zones. A close-up of the boundary between the North and Central zones is shown in Figure 14, and it also serves as the northern boundary for the Riding Area. The boundary is delineated by a fence line that trends west-east in zig-zag fashion, which then follows along the northern boundary of a sand-fencing area, and then trends eastward along N 35.0794° latitude to the eastern boundary of the ODVRA. On the western side, the boundary follows the park fence line heading north to the mouth of Arroyo Grande Creek.

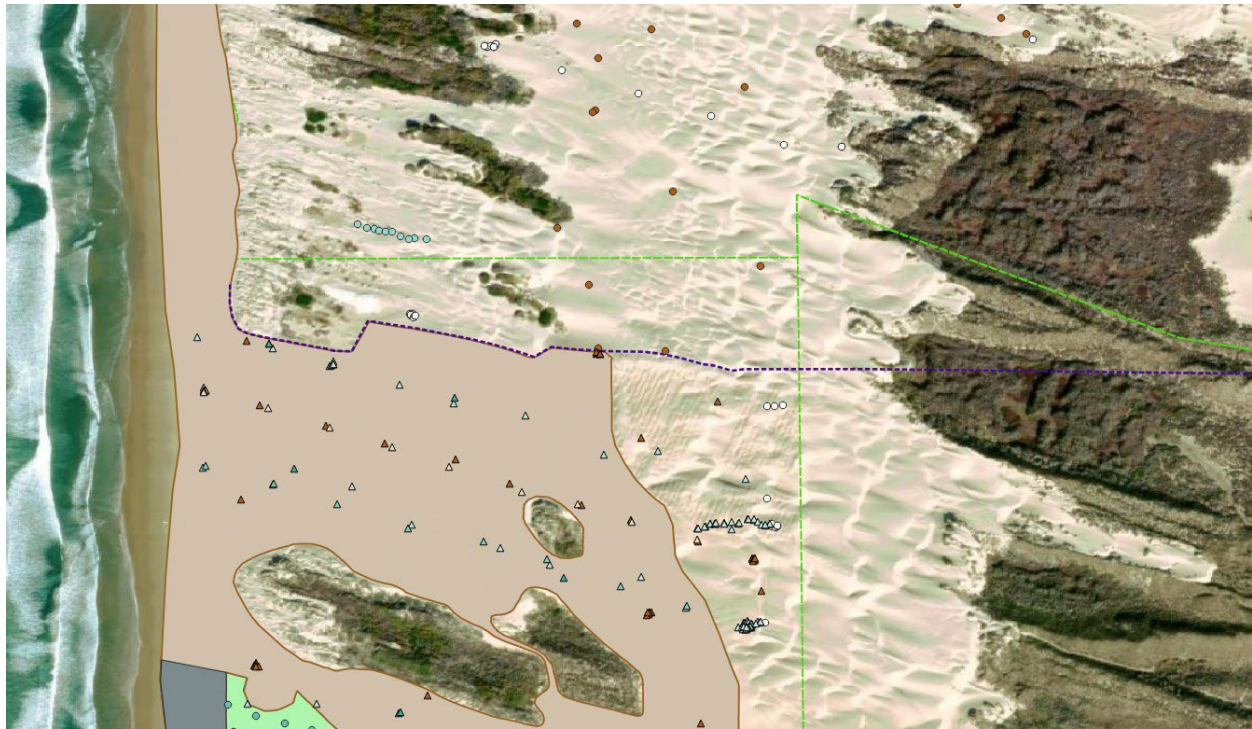


Figure 14: Proposed boundary line (purple dashed line) between the North and Central zones for the Non-Riding Area, which also delineates the northern boundary of the Riding Area. Refer to Figure 12 for location, and see Figure 5 for definition of symbols.

A close-up of the boundary between the NRA Central and NRA South is shown in Figure 15. This boundary begins on the beach and follows the fence line along the southern margin of the Plover Exclosure. It then transitions to the fence line delineating the southern margin of the Riding Area (RA Central-South), and from the most southerly point of the Riding Area takes a straight line to the nearest corner of the ODSVRA boundary and continues east along the park boundary through a thickly vegetated area.

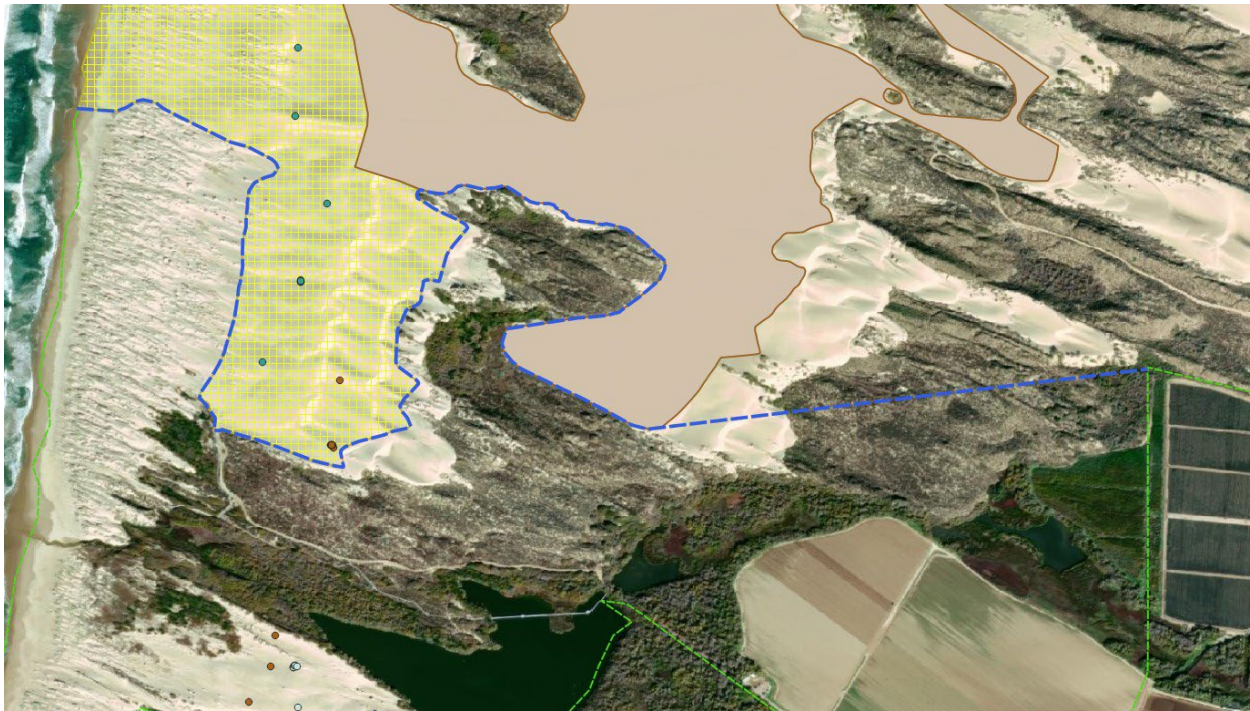


Figure 15: Proposed boundary line (dashed blue line) between NRA Central and NRA South zones, which also delineates the southern boundary of the Riding Area. Refer to Figure 12 for location, and see Figure 5 for definition of symbols.

A close-up of the FRA, the northern portion of the PE, and the Seasonal Exclusion (SE) area is presented in Figure 16. Also shown are some of the vegetation islands. All these zones are defined by GIS shapefiles managed by CDPR (T. Carmona, personal communication), and each of them is assigned a separate emissivity relation (as described below).

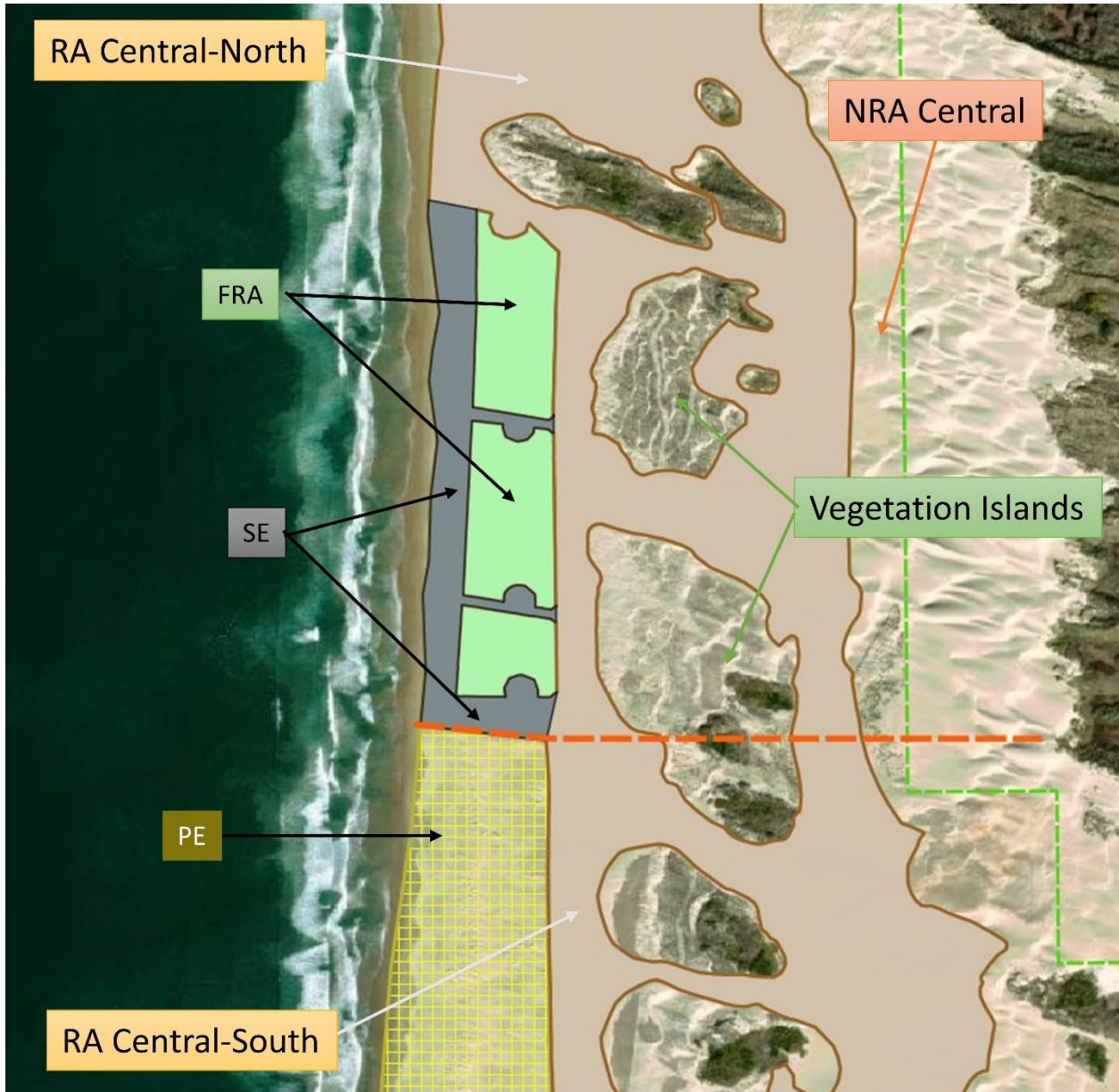


Figure 16: Outlines of the Foreduene Restoration Area (FRA), Plover Exclusion (PE), and the Seasonal Exclusion (SE) areas. The Riding Area is shown in tan color. Refer to Figure 12 for location.

The excess emissions framework proposed by SAG (SAG Memo – Framework for Assessing “Excess Emissions” of PM₁₀ from the Oceano Dunes, January 30, 2023) identifies the need to develop emissions grids for various modeling scenarios. This requires development of emissivity relations for each of the zones and sub-regions identified above, based on PI-SWERL measurement that are clustered or pooled accordingly.

For Current (2023) Conditions, it is recommended that the ODSVRA area be subdivided into nine zones (Figure 17), as follows:

1. Non-Riding Area North Zone
2. Non-Riding Area Central Zone
3. Non-Riding Area South Zone
4. Riding Area Central-North Sub-Region
5. Riding Area Central-South Sub-Region
6. Foredune Restoration Area (FRA)
7. Plover Exclosure (PE)
8. Seasonal Exclosures (SE)
9. Vegetated Areas (VEG)

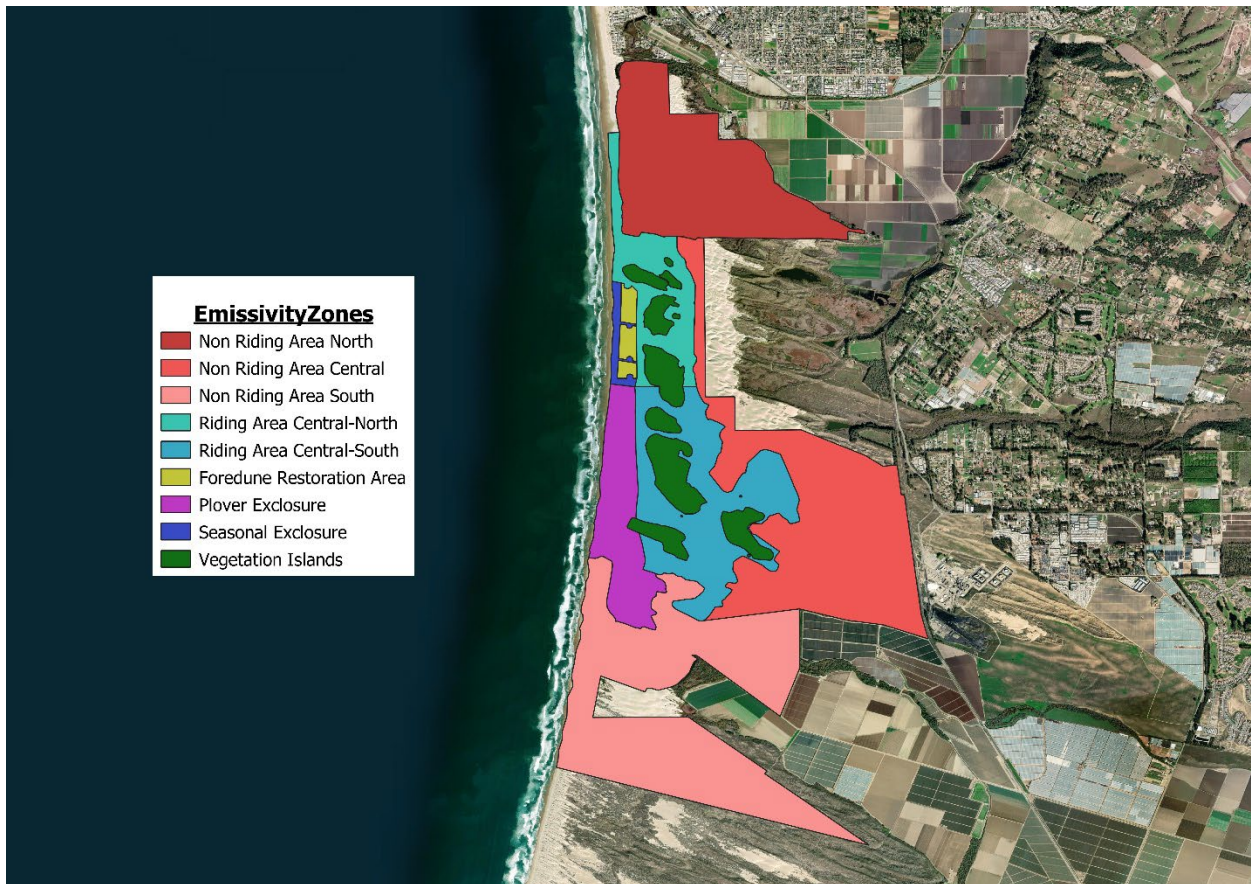


Figure 17: Emissivity zone polygons proposed for modeling the Current (2023) Conditions scenarios.

For the Pre-Disturbance (1939) scenario, it is recommended that the ODSVRA area be subdivided into three large NRA zones (North, Central, and South), as delineated by the boundaries shown in Figure 14 (between North and Central) and Figure 15 (between Central and South). Each of the three zones (Figure 18) will have a different emissions relation. The North zone is essentially the same as the Dune Preserve, which has not had OHV access for a long time. Similarly, the South zone encompasses the Oso Flaco area for which there has been no recent riding allowed. The Central zone, which currently has a mix of zones and riding access, will be classified in its entirety as "non-riding" for the pre-disturbance scenario, and only non-riding data from NRA Central will be used to characterize the emissivity relation. The 1939 vegetation cover mask developed by UCSB should be applied to this modeling scenario, yielding four distinct modeling zones (North, Central, South, Vegetation) all of which have non-riding characteristics.

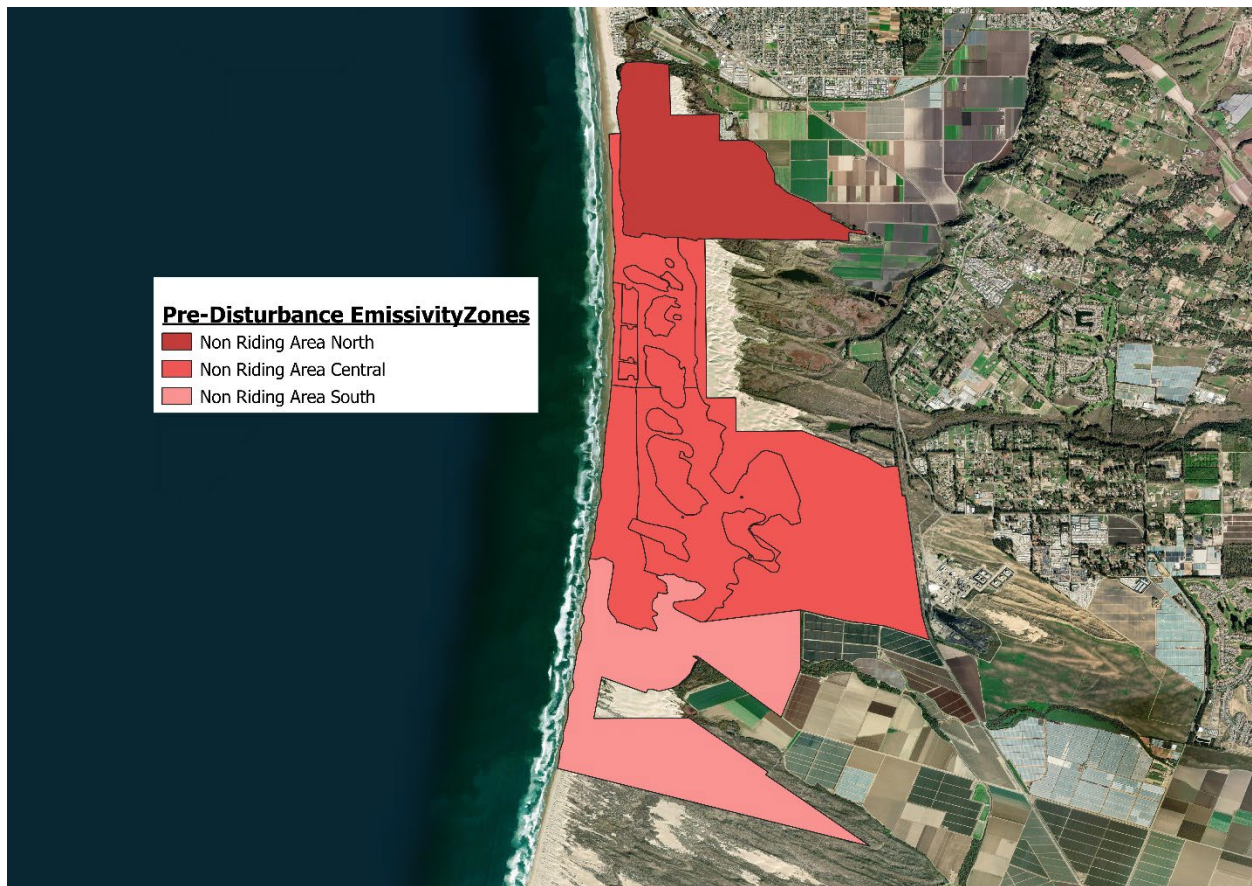


Figure 18: Emissivity zone polygons proposed for modeling the Pre-Disturbance (1939) scenarios. Vegetation cover mask to be superimposed.

Emissivity Curves

For each of the proposed zones and sub-regions identified above, emissivity relations will need to be assigned for purposes of modeling. These relations take the form of a power function:

$$F = a u_*^b$$

where F is the emissive flux ($\text{mg m}^{-2} \text{s}^{-1}$), u_* is shear velocity (m s^{-1}), a and b are coefficients from regression analysis of the PI-SWERL results for the three rotational speeds (Etyemezian et al., 2007). Such emissivity relations are deemed to be representative of the entire zone or sub-region, regardless of intra-area variations in surface characteristics (e.g., texture, mineralogy, slope, aspect, moisture content, degree of disturbance). Accounting for all such micro-scale controls is logistically impractical. Fortunately, there are a very large number of PI-SWERL measurements across the entire park area, making a statistical approach viable.

In past modeling efforts, emissivity grids were developed for both the 2013 and then the 2019 PI-SWERL measurement campaigns using a spatial interpolation algorithm superimposed on a 20 m by 20 m grid for the entire modeling domain. Each grid cell was given a different emissivity relation based on the spatially interpolated emissivity surface derived from the PI-SWERL measurements at unevenly distributed point locations. The proposal for moving forward is to define emissivity relations for each of the zones and sub-regions rather than for the 20 m by 20 m grid used earlier. Since each of the zones and sub-regions includes multiple measurements, a statistical approach implies using some measure of central dispersion (e.g., mean, mode, median) to quantify a representative emissivity value for each of the RPM speeds (shear velocities) of the PI-SWERL measurements.

Figure 19 shows two characteristic data distributions based on all the measurements (2013-2022) in the Central-North and Central-South Sub-Regions of the Riding Area. It is clear that the distributions are heavily skewed, with a large number of measurements falling at the low end of the emissivity range and a handful of measurements at the extreme high end of the emissivity range. Tests for normality consistently yield negative results, and as a consequence, standardized parameters used to describe Gaussian distributions (e.g., mean, standard deviation) are not strictly applicable.

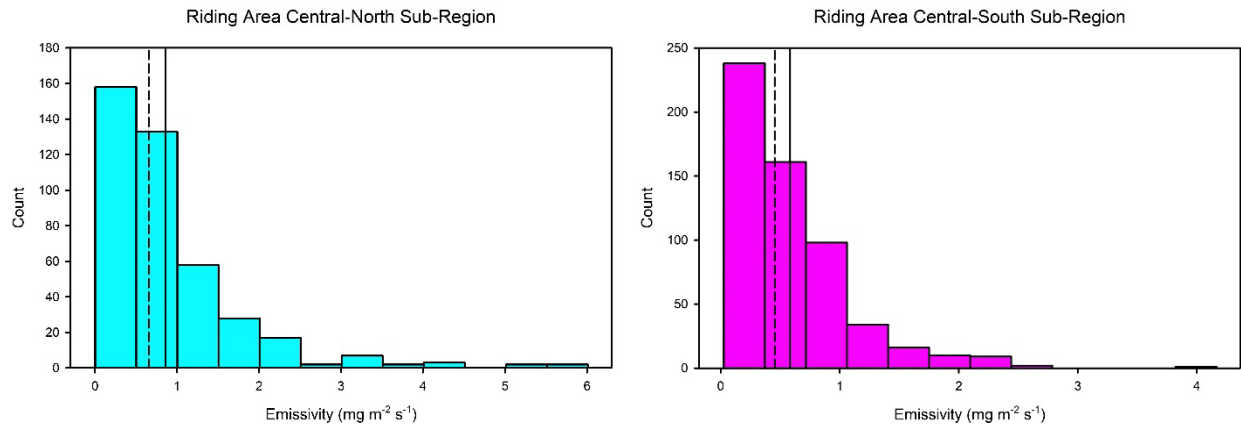


Figure 19: Histograms of PI-SWERL emissivities (Hi-RPM setting) for Central-North Sub-Region (left) and Central-South Sub-Region (right) of the Riding Area for all measurements from 2013 to 2022. Solid vertical line is the arithmetic mean; dashed vertical line is the median.

Although non-parametric statistics typically have reduced explanatory power, **it is recommended that future emissivity relations be based on the median** rather than the mean. The median is defined as the 'middle' value of the distribution, which is arguably more representative of the typical emissivity because it is not influenced by a few extreme values as is the mean. Figure 19 indicates that for the PI-SWERL data, the median is marginally smaller than the mean, although in some cases the mean can be considerably larger when skewed by a few measurements with extremely large emissivity values. This difference between using the median rather than the mean will yield updated values for modeled PM₁₀, and when applied to both the pre-disturbance and present conditions, it will facilitate a direct comparison of emissions for purposes of assessing the effectiveness of dust control measures.

The following recommendations are made in regard to assigning emissivity curves to the various zones and sub-regions:

Current (2023) Conditions Scenarios

<i>Zone or Sub-Region</i>	<i>Emissivity curves based on data from...</i>
NRA North	All 2013-2022 PI-SWERL measurements located in NRA North Zone
NRA Central	All 2013-2022 PI-SWERL measurements located in NRA Central Zone (not including FRA, PE, SE)
NRA South	All 2013-2022 PI-SWERL measurements located in NRA South Zone
RA Central-North	All 2013-2022 PI-SWERL measurements located in RA Central-North Sub-Region
RA Central-South	All 2013-2022 PI-SWERL measurements located in RA Central-South Sub-Region
FRA	Only 2022 PI-SWERL measurements located in the FRA
PE	Only 2022 PI-SWERL measurements located in the PE
SE	Weighted average of riding and non-riding measurements in SE areas (see below for details)

Pre-Disturbance (1939) Scenario

<i>Zone or Sub-Region</i>	<i>Emissivity curves based on data from...</i>
North (same as NRA North)	All 2013-2022 PI-SWERL measurements located in NRA North Zone
Central (same as NRA Central but also including footprint of RA areas between the north and south boundaries)	All 2013-2022 PI-SWERL measurements located in NRA Central Zone (not including FRA, PE, SE)
South (same as NRA South)	All 2013-2022 PI-SWERL measurements located in NRA South Zone

Note that for both the Current Conditions and Pre-Disturbance Scenarios, **the recommendation is to take advantage of the complete set of PI-SWERL measurements collected between 2013 and 2022**. Despite 2013 being an exceptionally dry year with demonstrably larger emissivity values (refer to discussion of Figures 1, 3 and 7), such dry years are part of the normal climatology of the region, and prolonged droughts are projected to become more frequent in the future. There is no defensible reason to exclude these data from consideration, and they help to

define the natural variability in the system, which should be accounted for when considering model uncertainty. Similarly, there are no defensible reasons for excluding any of the other PI-SWERL measurements (e.g., inordinately small or large emissivity) because they have been thoroughly quality controlled for errors associated with instrumental failure and transcription/coding inaccuracies by DRI personnel.

Table 4 provides the results for the emissivity relations developed for the Non-Riding and Riding Areas as well as the Foredune Restoration Area and Plover Exclosure area, based on the recommendations presented above. Graphic renditions of the data and power relations are shown in Figure 20. The same axis scaling is used for quick visual comparison, and it is apparent that the RA Central-North sub-region has the largest median emissivity. Interestingly, the RA Central-South sub-region has median emissivity that are not too dissimilar from the NRA North zone and NRA South zone, despite OHV restrictions in the latter two zones. The PE and FRA have the smallest median emissivity.

Table 4: Data used in developing emissivity relations. Power function coefficients (a, b) are shown at the bottom.

	Non-Riding Areas			Riding Areas		FRA	PE
	North	Central	South	Central-North	Central-South		
n =	111	221	67	403	574	110	23
u* (m s⁻¹)							
0.381	0.039	0.021	0.001	0.094	0.024	0.006	0.003
0.534	0.307	0.193	0.142	0.640	0.432	0.068	0.032
0.607	0.932	0.610	0.388	1.349	0.964	0.192	0.107
F = a (u*)^b							
a	66.376	51.649	20.786	24.340	24.395	10.710	11.416
b	8.547	8.893	7.972	5.795	6.466	8.060	9.355
r ²	.999	.999	.999	1.000	0.999	1.000	1.000

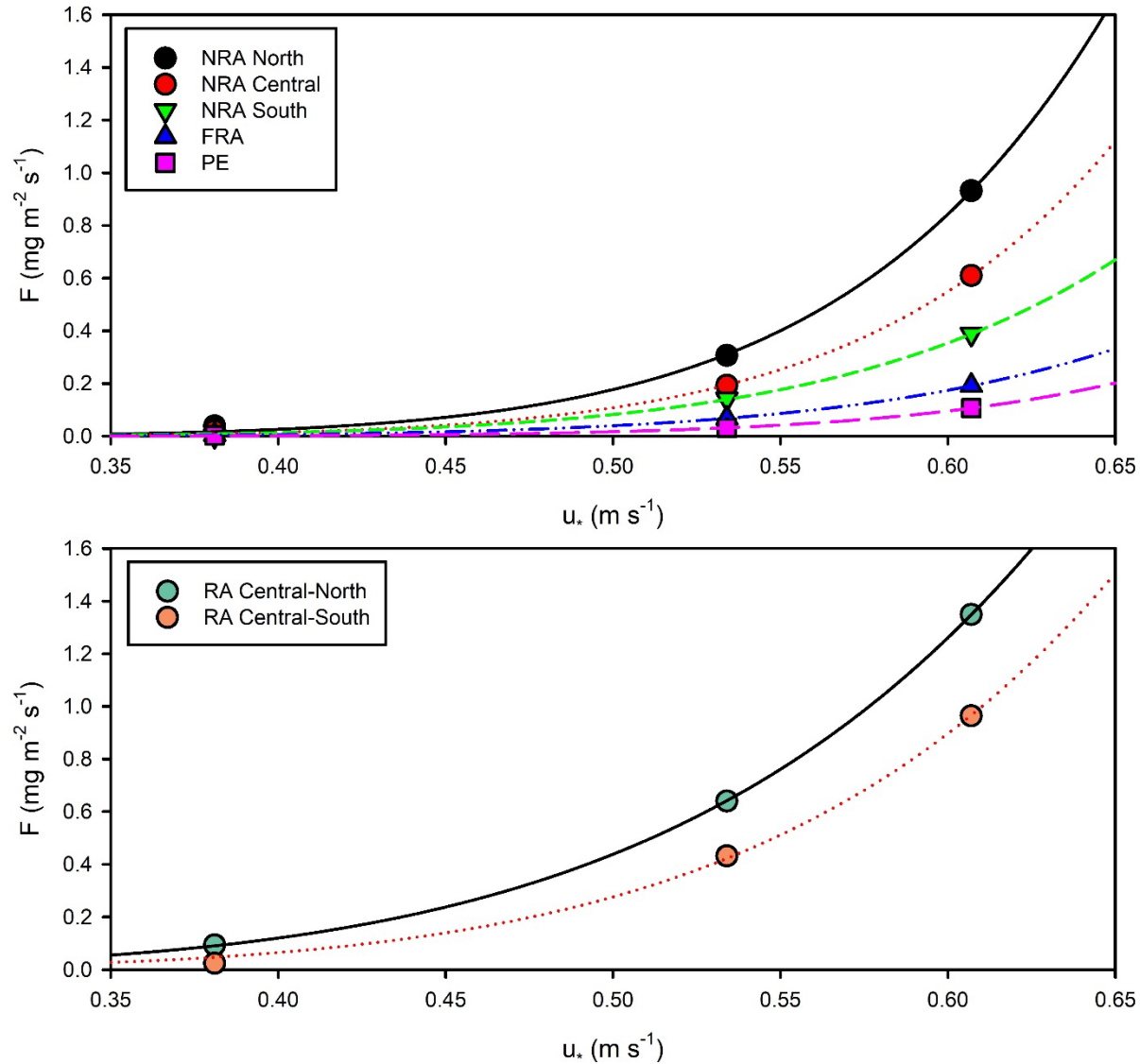


Figure 20: Emissivity relations for various zones in future modeling scenarios. Refer to Table 4 for details.

As mentioned previously, the Seasonal Exclusion areas require separate treatment because they are neither exclusively 'riding' nor 'non-riding.' There are two sub-zones within the SE area: (1) the narrow beach strip that lies to the west of the FRA; and (2) two access corridors that divide parts of the FRA and another access corridor between the PE and FRA (see Figure 16). The beach strip is closed to OHV use between March 1 and September 30, but accessible for OHV recreational use between October 1 and February 28. The corridors are managed similarly with the exception of the eastern entry areas that provide year-around rider access to toilet facilities.

A total of 69 PI-SWERL measurements were taken along the beach and corridor areas on September 30, 2022, which is at the end of exclusion period. Thus, these measurements are thought to be characteristic of the sand surface at the conclusion of the non-riding season after a

7-month period of continual adjustment. Some of these measurements were made in the year-around entry areas to the toilets and therefore are considered to be characteristic of the riding period. Several other measurements were made in corridors where it was noted that there had been recent disturbance of the surface by bulldozers as part of regular park maintenance. Therefore, of the 69 PI-SWERL measurements made in the SE area, 24 are classified as 'riding' whereas 45 are considered to be representative of 'non-riding' conditions. The 'riding' measurements were supplemented with another 34 measurements that were taken in the footprint of the SE area between 2013 and 2019 when OHV riding was allowed all year (i.e., before seasonal closure). These 34 measurements were extracted from the data set used to characterize RA Central-North using a GIS map to locate the relevant points. Table 5 presents the data and power function exponents, whereas Figure 21 shows the curves in graphical form.

Because there is a 'riding' period and a 'non-riding' period, each with different emissivity relations, it is necessary, for the purposes of modeling, to combine these to create a single curve. The simplest approach is to average the median values from both periods for each of the shear velocity increments, and then to develop a third relation based on the average of the medians. The results from this approach are also shown in Table 5 and Figure 21. Alternative approaches to yield a weighted average were explored using relaxation and ramp-up factors in an attempt to quantify the adjustments taking place on the landscape as the surface transitions from a highly emissive surface at the end of the riding period (February 28) to a less emissive surface at the end of the non-riding period (September 30), and back when OHV access is again allowed. However, very little is known about how rapidly these transitions occur and how they are influenced by meteorological conditions. In the end, the results were not that different from the simple averaging approach, lying somewhere in the middle between the two relations defining the riding and non-riding periods, so the simplest averaging approach was adopted.

Table 5: Data used in developing emissivity relations for the Seasonal Exclusion area. Power function coefficients (a, b) are shown at the bottom.

	Riding Affected Period (2013-2022)	Non-Riding Period (Sep 2022)	Average
n =	58	45	2
u* (ms⁻¹)			
0.381	0.049	0.006	0.028
0.534	0.295	0.065	0.180
0.607	0.678	0.200	0.439
E = a(u*)^b			
a	15.875	15.450	13.042
b	6.322	8.709	6.798
r ²	.999	1.000	.999

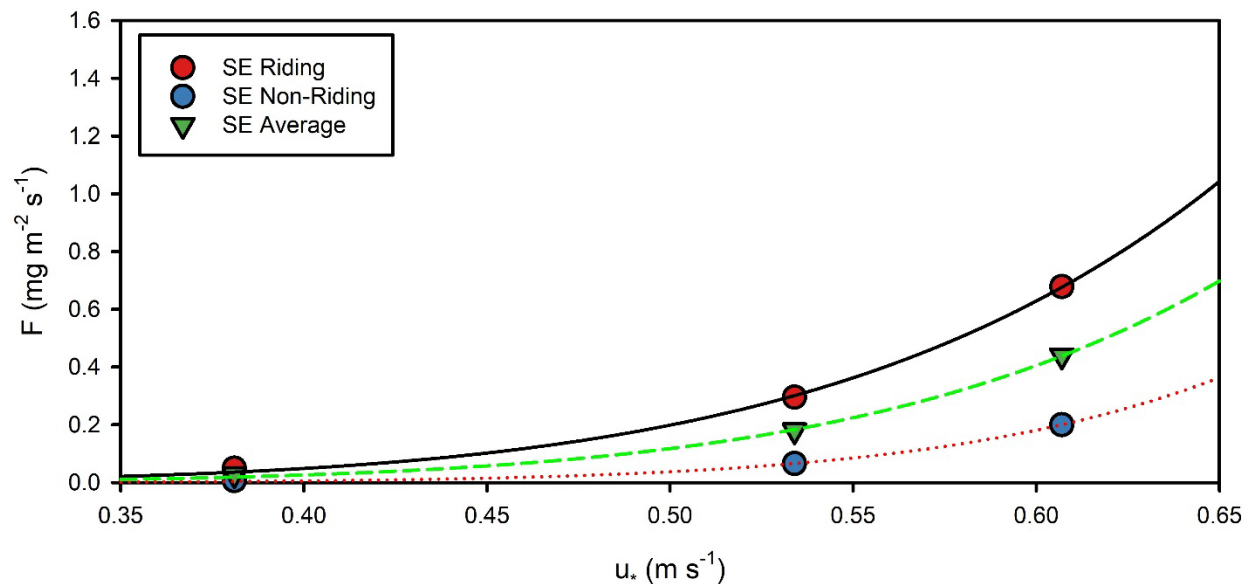


Figure 21: Emissivity relations for the Seasonal Exclusion area. Refer to Table 5 for details.

The pre-disturbance landscape would not have had zones equivalent to the FRA, PE, or SE, and there would have been limited influence from OHV riding. Therefore, **for the purposes of defining emissivity relations that characterize the Pre-Disturbance (1939) surface, it is recommended that all PI-SWRL measurements (2013-2022) from the NRA North zone be pooled to define a single power relation that applies to that zone only, and similarly so for the NRA Central zone and NRA South zone.** The rationale for not including any of the measurements from the FRA, PE, and SE areas is that these are all 'managed' landscapes in one way or another. For example, the FRA has six different treatments (species, planting densities, surface pre-treatments) and it is not known with any certainty how these varying surfaces, which are in continual stages of evolution, relate to a pre-disturbance condition. There is evidence from the air-photo reconstruction of the 1939 surface that foredunes were a component of the landscape, but given limited resolution and exposure in this early imagery, it is difficult to identify the exact extent of these areas, and there is no information on plant densities or heights from that time, which are critical factors in quantifying the sand-trapping and dust-retention characteristics of these former vegetated surfaces. More monitoring is needed over the next decade to better understand how the FRA will evolve and how the emissions characteristics will change. This does not undermine the use of the 2022 PI-SWRL measurements for the purposes of modeling the current (2023) landscape.

Similarly, the PE surface is a somewhat recently adjusted surface that is also managed for bird habitat, including the introduction of large woody debris that has, combined with emergent vegetation, lead to the development of appreciable incipient nebkha dune cover. One can imagine similar surfaces having evolved in the pre-disturbance environment after a major storm event that caused coastal inundation and erosion, for example. But it would likely still take a decade or longer for a disturbed sand surface to return to a completely natural state. This would involve multiple meteorological events across a range of speeds, directions, temperatures, and moisture conditions that serve to reorganize the sand surface in terms of texture, vegetation

cover, and dune development, but not yet reaching the stage of foredune development with mature plant communities. Thus, there is uncertainty as to how the measurements taken in the PE in 2022 might apply to a pre-disturbance landscape. The SE surface clearly has no counterpart in a pre-disturbance landscape given that it is seasonally subject to OHV disturbance, so these measurements will also not be used to characterize the pre-disturbance landscape.

Finally, all vegetated areas are treated identically in the current DRI model, with zero dust emissions, and it is recommended that this practice be followed in the near future for both the pre-disturbance and current conditions scenarios. This assumption is somewhat simplistic because there are areas in the ODSVRA that are densely vegetated (for which the assumption is clearly valid) and other areas that are sparsely vegetated or recently planted (for which there is likely to be some dust emission from open sand surfaces, especially under extreme wind events). However, in most of the managed areas where recent planting has taken place (with the exception of the FRA), it has been standard practice to spread straw on the surface, which prevents dust emissions for several years until the plants spread. In addition, there is relatively little understanding of how different plant species and assemblages prevent saltation and dust emissions even though it is generally appreciated that there is a dependency on plant height and stem density. Thus, given current uncertainty surrounding this issue, invoking a more complex dust emission scheme that is a function of plant characteristics across the treated surfaces is not yet viable nor recommended. The most expedient approach is to ensure that the shapefiles defining the vegetated areas truly reflect the geometry of the areas that are 'heavily' vegetated (with dense, mature vegetation covers or straw treatments with recently planted areas). These may not always follow enclosure fence lines, and the shapefiles will need to be continually updated, ideally using the UAS-derived surface cover maps.

CONCLUDING REMARKS

In respect of PM₁₀ emissions within the ODSVRA, Section 3.c. of the revised Stipulated Order of Abatement (SOA), filed on October 18, 2022, states that,

"Emissions shall be calculated using...a representative emissivity grid derived from PI-SWERL measurements as recommended by the SAG, ..."

In response to the second draft 2022 ARWP, the APCD's Conditional Approval letter (October 21, 2022) states that,

"Emission calculations in the 2023 ARWP shall be based on assumptions recommended by the SAG and preapproved, in writing, by the APCO."

The purpose of this memo is to satisfy both these requirements by presenting a detailed analysis of the PI-SWERL data collected to date and offer several recommendations that follow therefrom.

Appendix 1. Linear Theil Regression Analysis

Linear Theil regression (Theil, 1950; Wilcox, 2005) was performed on the PI-SWERL data to evaluate changes in emissivity over time. Theil regression is a non-parametric method that fits a line to data by computing the median of the slopes of all the possible combinations of pairs of data points. An advantage of the Theil regression is its insensitivity to outliers. The regression was performed on PI-SWERL data from 2013 through 2022, aggregated by percentile for both riding and non-riding areas (see Figures 1 and 3, respectively). Kendall tau statistics were used to determine statistical significance; a statistically significant trend was assumed at the 99% significance level ($p < 0.01$), meaning there is a 99% chance that the slope was not due to random chance.

Results for the three PI-SWERL speeds are shown in Tables A1 and A2 for the riding and non-riding areas, respectively. None of the trends were statistically significant ($p < 0.01$).

Table A1. Regression results for temporal trend analysis for PI-SWERL data for the **riding areas**. The percentile corresponds to the data distribution, the slope ($\text{mg m}^{-2} \text{s}^{-1} \text{day}^{-1}$) corresponds to data from 2013 through 2022, and p is the statistical significance. Three speeds (u^* is shear velocity) were used in the PI-SWERL instrument.

Percentile	$u^* = 0.381 \text{ ms}^{-1}$		$u^* = 0.534 \text{ ms}^{-1}$		$u^* = 0.607 \text{ ms}^{-1}$	
	slope	p	slope	p	slope	p
5	3.8E-07	0.02	-1.3E-05	1.00	-3.0E-05	0.62
10	4.1E-07	0.09	-4.3E-05	0.46	-3.5E-05	0.46
25	-4.5E-06	0.71	-5.5E-05	0.22	-4.3E-05	0.46
50	-1.7E-05	0.32	-1.1E-04	0.32	-2.2E-04	0.14
75	-5.5E-05	0.32	-1.9E-04	0.22	-2.2E-04	0.32
90	-1.0E-04	0.05	-2.8E-04	0.08	-5.2E-04	0.14
95	-1.3E-04	0.05	-3.7E-04	0.22	-3.2E-04	0.46

Table A2. Regression results for temporal trend analysis for PI-SWERL data for the **non-riding areas**. The percentile corresponds to the data distribution, the slope ($\text{mg m}^{-2} \text{s}^{-1} \text{day}^{-1}$) corresponds to data from 2013 through 2019, and p is the statistical significance. Three speeds (u^* is shear velocity) were used in the PI-SWERL instrument.

Percentile	$u^* = 0.381 \text{ ms}^{-1}$		$u^* = 0.534 \text{ ms}^{-1}$		$u^* = 0.607 \text{ ms}^{-1}$	
	slope	p	slope	p	slope	p
5	0	0.71	-2.5E-05	0.05	-5.7E-05	0.29
10	4.4E-07	0.64	-2.6E-05	0.02	-8.4E-05	0.10
25	-2.5E-06	0.54	-3.3E-05	0.05	-9.8E-05	0.05
50	-5.9E-06	0.29	-4.3E-05	0.18	-1.8E-04	0.18
75	-5.9E-06	0.18	-7.0E-05	0.18	-2.0E-04	0.29
90	-1.5E-06	0.88	-6.7E-06	0.65	-9.0E-05	0.45
95	3.2E-06	0.65	-5.2E-05	0.65	7.3E-05	0.65

References

Etyemezian, V., Nikolich, G., Ahonen, S., Pitchford, M., Sweeney, M., Purcell, R., Gillies, J., Kuhns, H., 2007. The Portable In-Situ Wind Erosion Laboratory (PI-SWERL): a new method to measure PM10 windblown dust properties and potential for emissions. **Atmos. Environ.** 41 (18), 3789–3796. <https://doi.org/10.1016/j.atmosenv.2007.01.018>.)

Mejia, J.F., Gillies, J.A., Etyemezian, V., Glick, R., 2019, A very-high resolution (20m) measurement-based dust emissions and dispersion modeling approach for the Oceano Dunes, California, **Atmospheric Environment** 218 (2019) 116977. <https://doi.org/10.1016/j.atmosenv.2019.116977>.

Thiel, H., 1950, A rank-invariant method of linear and polynomial regression analysis, **Proc. Kon. Ned. Akad. V. Wetensch. A.** 53, 386-392, 521-525, 1397-1412.

Wilcox, R., 2005, "10.2 Theil–Sen Estimator", **Introduction to Robust Estimation and Hypothesis Testing**, Academic Press, pp. 423–427, [ISBN 978-0-12-751542-7](https://doi.org/10.1016/B978-0-12-751542-7))